

## **Modelling crop growth and yield in palm oil cultivation**

*Christopher Teh Boon Sung<sup>1,\*</sup>, Cheah See Siang<sup>2</sup>, R.H.V. Corley<sup>3</sup>*

<sup>1</sup> *Faculty of Agriculture, Uni. Putra Malaysia, Serdang, Malaysia (christeh@yahoo.com)*

<sup>2</sup> *Sime Darby Research Sdn. Bhd., Banting, Malaysia*

<sup>3</sup> *Sime Darby Technology Centre, Serdang, Malaysia*

### **1. Introduction**

The first semi-mechanistic oil palm model is OPSIM (van Kraalingen, 1985). It was developed by taking into account some aspects oil palm's crop physiology and the physical processes and causal relationships between the environment and crop. OPSIM was later modified by Gerristma (1988) to have a more rigorous approach to estimate oil palm photosynthesis and by Dufrêne et al. (1990) to have their model (SIMPALM) rely much more on measured data of oil palm vegetative parameters. GPHOT, GPHOT2, and later OPRODSIM (Henson, 1989, 2000, 2009) were perhaps the most comprehensive at that period, as Henson's models progressively improved by including increasingly more effects and factors of oil palm growth and yield. They included aspects such as the effects of air vapor pressure deficit and available soil water on oil palm photosynthesis. Fitted relationships, based on measured data collected from various oil palm studies, were later included to better estimate oil palm root turnover, dry matter partitioning, and flower sex ratios. Since then, the development of new oil palm models have increased in frequency, such as WaNuLCAS (van Noordwijk et al., 2011), ECOPALM (Combres et al., 2013), and PALMSIM (Hoffmann et al., 2014). More recent oil palm models such as APSIM-Oil Palm (Huth et al., 2014), CLM-Palm (Fan et al., 2015), and CLIMEX-Oil Palm (Paterson et al., 2015) are actually components of a larger, more general modeling framework. The APSIM-Oil Palm, for instance, is one of the 30 sub-models for various crops, trees, and pastures under the APSIM model framework.

The purpose of this chapter is to discuss the development of a new oil palm growth and yield model called PySawit. There are several key aspects that differentiates PySawit from other models. First, PySawit attempts to model oil palm photosynthesis in a more rigorous manner based on the biochemical photosynthesis model by Collatz et al. (1991), a modification of the original photosynthesis model by Farquhar et al. (1980). Other oil palm models tend to use oil palm's radiation use efficiency of intercepted radiation (based on Beer's law) to convert the intercepted radiation into gross photosynthesis. Second, the microclimate environment within

and under the oil palm canopies is modeled by describing the soil-plant-atmosphere system of oil palm as a network of resistances in which latent and sensible heat fluxes from the soil and crop must traverse, akin to the flow of electrical current, driven by potential differences and impeded by a series of resistances (Shuttleworth and Wallace, 1985). The Shuttleworth-Wallace (SW) evapotranspiration model is an important extension of the Penman-Monteith model (Monteith, 1965) because the SW model allows the simultaneous heat fluxes from both soil and crop, unlike its predecessor that would only allow fluxes from either soil or crop but not both simultaneously. And third, PySawit is developed specifically for oil palm planted on a wide range of planting densities, from about 120 to 300 palms ha<sup>-1</sup>. The recent oil palm models such as APSIM-Oil Palm, CLM-Palm, and PALMSIM were validated only over a narrow planting density range of between 127 to 156 palms ha<sup>-1</sup>. The accuracy of the CLIMEX-Oil Palm, on the other hand, was not even validated. Moreover, most oil palm models, especially recent ones, have only been validated over a limited period of the oil palm growth stage (usually only when the oil palms have fully matured).

Consequently, the second purpose of this chapter is to discuss the evaluation of PySawit's accuracy when its predictions were compared with several measured parameters of growth and yield of oil palm from ages 1 to 19 yrs. These oil palm were planted with ten different planting densities, ranging from 122 to 296 palms ha<sup>-1</sup>, at an oil palm estate at Merlimau, Malaysia. The degree of agreement between PySawit's predictions and observations was evaluated by visual inspection of scatterplots between predictions and observations and by the use statistical goodness-of-fit indexes.

## **2. Theory and model development**

PySawit simulations are for crop production level 2, where the growth and yield of oil palm is limited only by weather conditions and water availability (de Witt and Penning de Vries, 1982). The model assumes the oil palm is growing under optimal nutrient levels and without any detrimental effects from pests, diseases, and weeds, and is managed following standard practices (such as pruning and mulching) by the oil palm industry.

PySawit comprises five core components: 1) meteorology, 2) photosynthesis, 3) energy balance, 4) soil water, and 5) crop growth. The meteorology component contains calculations pertaining to both daily and hourly meteorological elements such as air temperature, wind speed, humidity, solar irradiance, and rain. The photosynthesis component comprises calculations for determining the oil palm photosynthesis, and the energy balance component the various heat fluxes to determine the potential evapotranspiration and canopy temperature. The soil water component works out the soil water balance and the various water fluxes in the

soil layers to determine the amount of water available to the crop and the level of crop water stress, if any. The last component, crop growth, determines the crop maintenance and growth respirations, and the balance of assimilates from photosynthesis is then finally channeled for bunch production and yield.

## 2.1 Meteorology

Simulations begin at the meteorology component. PySawit requires only four daily meteorological properties: minimum and maximum air temperature ( $^{\circ}\text{C}$ ), wind speed ( $\text{m s}^{-1}$ ), and rain (mm) to estimate the various instantaneous meteorological properties such as solar irradiance, wind speed, air temperature, vapor pressure, and humidity. Routine information on the site's local solar hour of sunrise  $t_{sr}$  and sunset  $t_{ss}$ , day length  $DL$  (hours), solar inclination  $\theta$  (solar angle from vertical) (radians), extraterrestrial solar irradiance  $I_{et}$  ( $\text{W m}^{-2}$ ), relative humidity  $RH$  (%), and saturated vapor pressure (mbar) can be determined from Goudriaan and van Laar (1994).

Instantaneous total solar irradiance comprises two components: direct and diffuse components, where the direct component arrives from a single direction (the solar position), whereas the diffuse component arrives from all directions due to scattering and reflection from various surfaces in the environment. Calculations from Liu and Jordan (1960) are followed to determine both these solar radiation components as

$$I_t = I_{dr} + I_{df} \quad (10.1a)$$

$$I_{dr} = I_{et} \cdot \tau^m \quad (10.1b)$$

$$I_{df} = 0.3(1 - \tau^m)I_{et} \quad (10.1c)$$

where  $I_t$ ,  $I_{dr}$ , and  $I_{df}$  are the instantaneous total, direct, and diffuse solar irradiance, respectively (all in  $\text{W m}^{-2}$ );  $\tau$  is the sky clearness index (or atmospheric transmittance, the ratio between  $I_t$  and  $I_{et}$ ); and  $m$  is the optical mass number. The optical mass number  $m$  is determined from Campbell and Norman (1998) as

$$m = P_a / (101.3 \cos \theta) \quad (10.2)$$

where  $P_a$  is the atmospheric pressure (kPa), assumed constant at 101 kPa.

Dimas et al. (2011) showed that  $\tau$  can be estimated from relative humidity ( $RH$ ) and in turn be used to calculate  $I_t$  and its components:  $I_{dr}$  and  $I_{df}$ . Hourly meteorological data for years 2015 and 2016 were obtained from weather stations located at five Malaysian oil palm estates: Bukit Selarong, Kedah (5.462824 °N, 100.597084 °E); Diamond Jubilee, Melaka (2.333333 °N, 102.483333 °E); Imam, Sabah (4.333333 °N, 117.833333 °E); Seri Intan, Perak (3.976583 °N, 100.9739 °E); and Ulu Remis, Johor (1.827778 °N, 103.461944 °E), where the following linear relationship between  $\tau$  and  $RH$  was derived:

$$\tau = 1.1857 - 0.0112RH \quad (10.3)$$

where  $RH$  is the relative humidity (%) (Fig. 10.1).

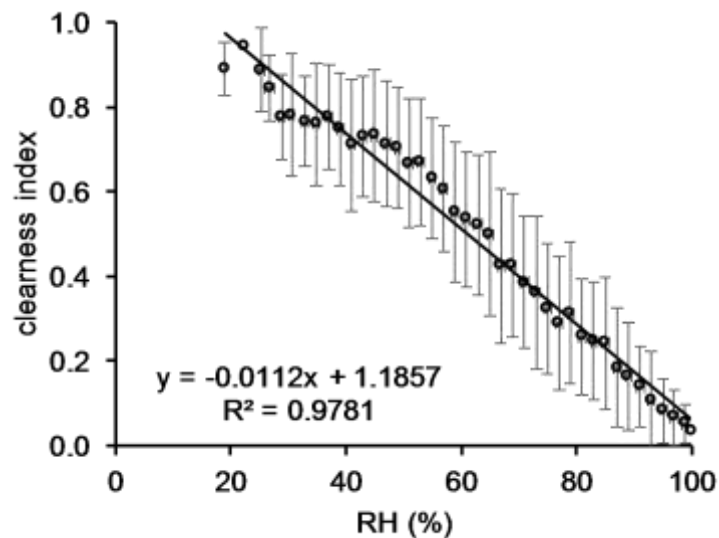


Figure 10.1. Linear relationship between measured relative humidity ( $RH$ ) and sky clearness index between 2015 to 2016 for five stations in Malaysia (N = 25548). Note: the bars represent one standard deviation.

The daily trend of instantaneous air temperature for these five stations were also observed to vary sinusously with time during the period between 1.5 hours after the time of minimum air temperature and time of sunset. Outside this period, air temperature was observed to change linearly with time. This trend can be accurately depicted by the following mathematical relationships according to Wilkerson et al. (1983) as

$$T_a = \begin{cases} T_{set} + \frac{(T_{min} - T_{set})(24 + t_h - t_{ss})}{(t_{sr} + 1.5) + (24 - t_{ss})} & t_h < (t_{sr} + 1.5) \\ T_{set} + \frac{(T_{min} - T_{set})(t_h - t_{ss})}{(t_{sr} + 1.5) + (24 - t_{ss})} & t_h > t_{ss} \\ T_{min} + (T_{max} - T_{min})\sin\left[\frac{\pi(t_h - t_{sr} - 1.5)}{t_{ss} - t_{sr}}\right] & otherwise \end{cases} \quad (10.4a)$$

$$T_{set} = T_{min} + (T_{max} - T_{min})\sin\left[\frac{\pi(t_{ss} - t_{sr} - 1.5)}{t_{ss} - t_{sr}}\right] \quad (10.4b)$$

where  $T_a$  is the air temperature;  $T_{min}$  and  $T_{max}$  are the minimum and maximum air temperature, respectively; and  $T_{set}$  is the air temperature at the time of sunset ( $t_{ss}$ ). All temperatures are in °C.

The dew point temperature  $T_{dew}$  for these five stations were rather constant throughout the year, with a mean of 23 °C. This value is within the range reported by Mohd. Desa and Rakhecha (2006), who also observed a rather constant dew point temperature between 20 to 24 °C for 24 towns across Malaysia for the period between 1994 and 2003.

Knowing the dew point temperature  $T_{dew}$  enables the determination of air vapor pressure according to Ephraïm et al. (1996) as

$$e_a = 6.1078 \exp\left(\frac{17.269T_{dew,cal}}{T_{dew,cal} + 237.3}\right) \quad (10.5)$$

where  $e_a$  is the air vapor pressure (mbar); and  $T_{dew,cal}$  is the calibrated dew point temperature (°C), where it should be lower than the current air temperature,  $T_a$ .

$$T_{dew,cal} = \text{MIN}[[T_a, T_{dew}]] \quad (10.6)$$

where  $\text{MIN}[[n_1, n_2, \dots, n_n]]$  is the minimum function, returning the smallest of the enclosed values.

The instantaneous wind speed typically varies sinusously within the day as

$$u = \text{MAX} \left[ \left[ u_{min}, u_{min} + (u_{max} - u_{min})\sin\left[\frac{\pi}{DL}(t_h - t_{sr} - 1.5)\right] \right] \right] \quad (10.7)$$

where  $u$  is the wind speed ( $\text{m s}^{-1}$ );  $u_{max}$  and  $u_{min}$  are the maximum and minimum wind speed for the day, respectively ( $\text{m s}^{-1}$ ); and  $MAX[[n_1, n_2, \dots, n_n]]$  is the maximum function, returning the largest of the enclosed values. The mean daily minimum and maximum wind speed can be estimated by the following equations, developed by fitting the best function to the measured hourly wind speed data for several towns in Malaysia from 1982 to 1991 (Sopian et al., 1995):

$$u_{min} = 0.5591u_d^{1.25} \quad (10.8)$$

$$u_{max} = 1.7976u_d^{0.75} \quad (10.9)$$

where  $u_d$  is the mean daily wind speed ( $\text{m s}^{-1}$ ).

## 2.2 Photosynthesis

The photosynthesis model by Collatz et al. (1991), which is based on Farquhar et al. (1980), is adapted to determine the amount of  $\text{CO}_2$  assimilated by the oil palm canopies, where gross leaf  $\text{CO}_2$  assimilation is limited by the lowest of the three potential assimilation rates due to Rubisco, light, and sink:

$$\Lambda_{sl/sh} = MIN[[v_c, v_{q,sl/sh}, v_s]] \quad (10.10)$$

where  $\Lambda_{sl/sh}$  is the gross leaf  $\text{CO}_2$  assimilation for either sunlit (subscript  $sl$ ) or shaded ( $sh$ ) leaves;  $v_c$ ,  $v_q$ , and  $v_s$  are the Rubisco-, light-, and sink-limited assimilation rates, respectively. All assimilation rates are in  $\mu\text{mol CO}_2 \text{ m}^{-2} \text{ leaf s}^{-1}$ .

Leaf  $\text{CO}_2$  assimilation rate is scaled up to canopy level, following Campbell and Norman (1998), by

$$\Lambda_{canopy} = \Lambda_{sl}L_{sl} + \Lambda_{sh}L_{sh} \quad (10.11)$$

where  $\Lambda_{canopy}$  is the gross canopy  $\text{CO}_2$  assimilation ( $\mu\text{mol CO}_2 \text{ m}^{-2} \text{ ground s}^{-1}$ ); and  $L_{sl}$  and  $L_{sh}$  are the sunlit and shaded leaf area index, respectively (both in  $\text{m}^2 \text{ leaf m}^{-2} \text{ ground}$ ).

Eq. 10.11 is integrated over sunrise ( $t_{sr}$ ) to sunset ( $t_{ss}$ ) to determine the daily gross canopy photosynthesis as

$$\Lambda_{canopy,d} = \frac{1.08}{PD} \int_{t_{sr}}^{t_{ss}} \Lambda_{canopy} dt \quad (10.12)$$

where  $\Lambda_{canopy,d}$  is the daily gross photosynthesis (converted to kg CH<sub>2</sub>O palm<sup>-1</sup> day<sup>-1</sup>); and  $PD$  is the planting density (palms ha<sup>-1</sup>). Integration is by the numerical Gaussian integration method, where five points over the diurnal period (from sunrise to sunset) are selected, and for each selected hour, the gross canopy CO<sub>2</sub> assimilation is calculated (Teh, 2006).

The following sub-sections describe the meaning and calculations of the various parameters in Eq. 10.10 and 10.11.

### 2.2.1 Rubisco-limited assimilation ( $v_c$ )

Rubisco-limited leaf CO<sub>2</sub> assimilation rate  $v_c$  is determined by

$$v_c = \frac{V_{cmax}(C_i - \Gamma^*)}{K_c(1 + O_a/K_o) + C_i} \quad (10.13)$$

where  $K_c$  is the Michaelis-Menten constant for CO<sub>2</sub> (μmol CO<sub>2</sub> mol<sup>-1</sup> air);  $K_o$  is the Michaelis-Menten constant for O<sub>2</sub> (μmol O<sub>2</sub> mol<sup>-1</sup> air);  $\Gamma^*$  is the CO<sub>2</sub> compensation point (μmol CO<sub>2</sub> mol<sup>-1</sup> air);  $O_a$  is the ambient O<sub>2</sub> concentration in air (210000 μmol O<sub>2</sub> mol<sup>-1</sup> air);  $C_i$  is the intercellular CO<sub>2</sub> concentration (μmol CO<sub>2</sub> mol<sup>-1</sup> air); and  $V_{cmax}$  is the maximum Rubisco capacity rate (μmol CO<sub>2</sub> m<sup>-2</sup> leaf s<sup>-1</sup>). The CO<sub>2</sub> compensation point  $\Gamma^*$  (CO<sub>2</sub> concentration at the point where assimilation is zero) is determined by

$$\Gamma^* = 0.5 O_a / \tau \quad (10.14)$$

where  $\tau$  is the CO<sub>2</sub>/O<sub>2</sub> specificity factor (μmol O<sub>2</sub> μmol<sup>-1</sup> CO<sub>2</sub>). For C3 plants like oil palm,  $\tau$  indicates the level of competition between O<sub>2</sub> and CO<sub>2</sub> substrates for the Rubisco enzyme.

Most of the parameters in Eq. 10.13 are temperature-dependent and must be corrected for foliage temperature ( $T_f$ ). Correction is by multiplying their values at 25 °C with their corresponding Q<sub>10</sub> temperature coefficients (Table 10.1). Q<sub>10</sub> is a measure of the rate of change of a given biochemical activity due to the increase in the temperature by 10 °C.

Table 10.1. Values of temperature-dependent photosynthesis parameters  $\xi_{(25)}$  at 25 °C. Except for  $V_{cmax(25)}$ , all values are from Bernacchi et al. (2001, 2002), and they are general values for C3 plants.

$\xi_{(25)}$	Description	Unit	Value	$Q_{10,\xi}$
$K_c(25)$	Michaelis-Menten constant for CO <sub>2</sub>	$\mu\text{mol CO}_2 \text{ mol}^{-1} \text{ air}$	270	2.786
$K_o(25)$	Michaelis-Menten constant for O <sub>2</sub>	$\mu\text{mol O}_2 \text{ mol}^{-1} \text{ air}$	165000	1.355
$\tau(25)$	CO <sub>2</sub> /O <sub>2</sub> specificity factor	$\mu\text{mol O}_2 \mu\text{mol}^{-1} \text{ CO}_2$	2800	0.703
$V_{cmax(25)}$	Maximum Rubisco capacity rate	$\mu\text{mol CO}_2 \text{ m}^{-2} \text{ leaf s}^{-1}$	81	2.573

Temperature correction for these parameters follows this general form:

$$\xi = \xi_{(25)} \times Q_{10,\xi}^{(T_f-25)/10} \quad (10.15)$$

where  $\xi_{(25)}$  is the parameter value at 25 °C;  $T_f$  is the canopy temperature (°C); and  $Q_{10,\xi}$  is the relative change in parameter  $\xi$  for every 10 °C change (Table 10.1). However,  $V_{cmax}$  has to be additionally corrected for foliage temperatures greater than 40 °C, because after which the Rubisco enzyme degrades, causing a rapid decline in CO<sub>2</sub> assimilation:

$$V_{cmax} = \frac{V_{cmax(25)} \times 2.573^{(T_f-25)/10}}{1 + \exp[0.29(T_f - 40)]} \quad (10.16)$$

$V_{cmax(25)}$  for oil palm is determined to slightly decline with tree age, from a mean of 96 to 86  $\mu\text{mol CO}_2 \text{ m}^{-2} \text{ leaf s}^{-1}$  between palm ages 1 to 2 yrs, then thereafter remaining rather stable at about 81  $\mu\text{mol CO}_2 \text{ m}^{-2} \text{ leaf s}^{-1}$  (Fig. 10.2). The relationship between oil palm  $V_{cmax(25)}$  and tree age can be described by the following linear equation:

$$V_{cmax(25)} = 89.508 - 0.0015age \quad (10.17)$$

where  $age$  is the tree age (in days).

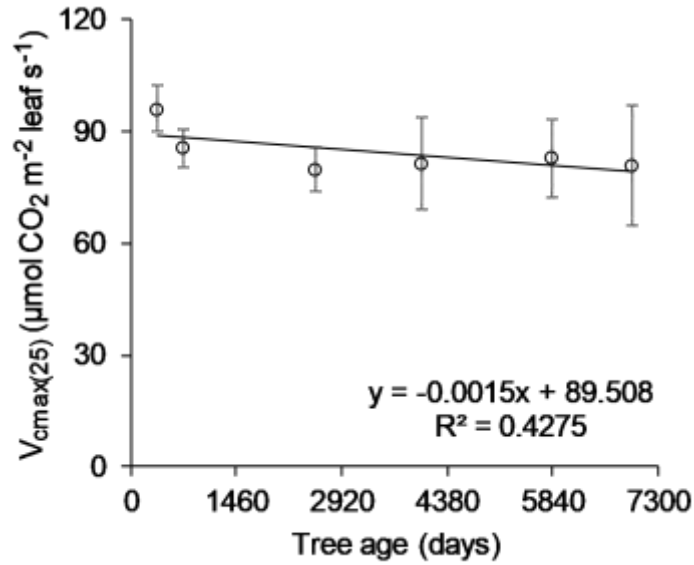


Figure 10.2. Change in the maximum Rubisco capacity rate  $V_{cmax(25)}$  with oil palm tree age. Leaf gas exchanges for 1 to 19 yrs palm trees were measured (N = 48) (Long and Bernacchi, 2003) using the TPS-2 Portable Photosynthesis System (PP Systems International, Inc., Amesbury, US), and based on the gas exchange data,  $V_{cmax(25)}$  were estimated based on Sharkey et al. (2007) and Sharkey (2005). Note: the bars represent one standard deviation.

Our measured  $V_{cmax(25)}$  is between 5 to 20% smaller than that used by Fan et al. (2015) for their oil palm growth simulations. Fan et al. (2015) used a constant  $V_{cmax(25)}$  of  $100.7 \mu\text{mol CO}_2 \text{ m}^{-2} \text{ leaf s}^{-1}$ , a value they had calculated based on the leaf N content and specific leaf area for crops in general (not specifically based on oil palm leaves).

The intercellular  $\text{CO}_2$  concentration ( $C_i$ ) can be determined from its relationship with ambient  $\text{CO}_2$  concentration ( $C_a$ ) (both concentrations expressed as  $\mu\text{mol CO}_2 \text{ mol}^{-1} \text{ air}$ ) and vapor pressure deficit in the leaves by the following equation by Yin and van Laar (2005):

$$C_i/C_a = 1 - (1 - \Gamma^*/C_a)(a + bD_{leaf}) \quad (10.18)$$

where  $D_{leaf}$  is the leaf vapor pressure deficit (mbar), determined by

$$D_{leaf} = e_s[T_f] - e_a \quad (10.19)$$

where  $e_s[T_f]$  the saturated vapor pressure (mbar) at foliage temperature  $T_f(^{\circ}\text{C})$ ; and  $e_a$  is the air vapor pressure (mbar). Leaf measurements on various ages of oil palm trees (from 1 to 19 yrs) revealed that coefficients  $a$  and  $b$  are 0.0615 and 0.0213, respectively (Fig. 10.3).

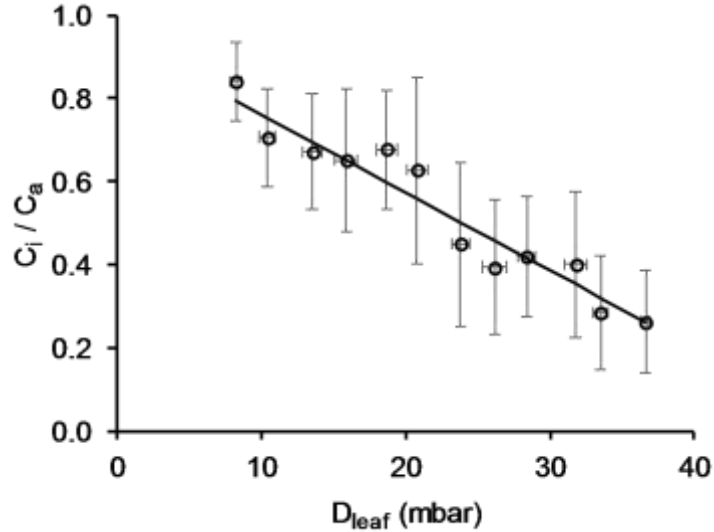


Figure 10.3. Decline in the ratio between intercellular CO<sub>2</sub> concentration ( $C_i$ ) and ambient CO<sub>2</sub> concentration ( $C_a$ ) with increasing leaf vapor pressure deficit ( $D_{leaf}$ ) for 1 to 19 yr oil palm trees (N = 654). Leaf gas exchanges were measured based on Long and Bernacchi (2003) using the TPS-2 Portable Photosynthesis System (PP Systems International, Inc., Amesbury, US). Note: the bars represent one standard deviation.

### 2.2.2 Light-limited assimilation ( $v_q$ )

Light-limited leaf CO<sub>2</sub> assimilation rate  $v_q$  is determined by

$$v_{q,sl/sh} = 0.8e_m Q_{sl/sh} (C_i - \Gamma^*) / (C_i + \Gamma^*) \quad (10.20)$$

where  $v_{q,sl/sh}$  is the light-limited leaf CO<sub>2</sub> assimilation rate ( $\mu\text{mol CO}_2 \text{ m}^{-2} \text{ leaf s}^{-1}$ ) for either sunlit (subscript  $sl$ ) or shaded ( $sh$ ) leaves;  $Q_{sl/sh}$  is the photosynthetically active radiation (PAR) flux densities absorbed by either sunlit or shaded leaves ( $\mu\text{mol m}^{-2} \text{ leaf s}^{-1}$ ); and  $e_m$  is the intrinsic quantum efficiency or yield ( $\mu\text{mol CO}_2 \mu\text{mol}^{-1} \text{ photons}$ ), taken as 0.051 for oil palm (Dufrêne and Saugier, 1993). Skillman (2008) reviewed ten studies that measured  $e_m$  of various C3 plants, and its mean ( $\pm$  s.e.) from these studies were  $0.052 \pm 0.003$  (N = 61).

According to Campbell and Norman (1998), there are four PAR flux components within the canopies, and they are the: 1) PAR irradiance for unintercepted beam *with* scattering  $Q_{p,dr}$  ( $\mu\text{mol photons m}^{-2} \text{ ground s}^{-1}$ ), 2) PAR irradiance for unintercepted beam *without* scattering  $Q_{p,dr,dr}$  ( $\mu\text{mol photons m}^{-2} \text{ ground s}^{-1}$ ), 3) PAR irradiance of *only* the scattered component

$Q_{p,dr,\alpha}$  ( $\mu\text{mol photons m}^{-2} \text{ leaf s}^{-1}$ ), and 4) mean diffuse PAR irradiance  $\overline{Q_{p,df}}$  ( $\mu\text{mol photons m}^{-2} \text{ leaf s}^{-1}$ ). Note that both  $Q_{p,dr,\alpha}$  and  $\overline{Q_{p,df}}$  are expressed based on a per unit leaf area (not per unit ground area). The scattered and diffuse irradiance on a unit horizontal ground area are assumed equal to their irradiance on a unit leaf area. These four PAR flux components can be calculated by

$$Q_{p,dr} = (1 - p_{dr})Q_{dr} \exp(-k_{dr}\omega\sqrt{0.8}L) \quad (10.21)$$

$$Q_{p,dr,dr} = (1 - p_{dr})Q_{dr} \exp(-k_{dr}\omega L) \quad (10.22)$$

$$Q_{p,dr,\alpha} = (Q_{p,dr} - Q_{p,dr,dr})/2 \quad (10.23)$$

$$\overline{Q_{p,df}} = (1 - p_{df})Q_{df} [1 - \exp(-k_{df}\sqrt{0.8}L)]/k_{df}L \quad (10.24)$$

where  $Q_{dr}$  and  $Q_{df}$  are the instantaneous direct and diffuse PAR irradiance, respectively (both in  $\mu\text{mol photons m}^{-2} \text{ ground s}^{-1}$ );  $p_{dr}$  and  $p_{df}$  are the canopy reflection coefficient for direct and diffuse PAR, respectively (both unitless);  $k_{dr}$  and  $k_{df}$  are the canopy extinction coefficients for direct and diffuse PAR, respectively (both unitless);  $\omega$  is the canopy clustering coefficient for discontinuous canopies (0 to 1); and  $L$  is the total leaf area index ( $\text{m}^2 \text{ leaf m}^{-2} \text{ ground}$ ).

The PAR irradiance components  $Q_{dr}$  and  $Q_{df}$  are determined by

$$Q_{dr} = I_{dr} \times 4.55 \times 0.5 \quad (10.25)$$

$$Q_{df} = I_{df} \times 4.55 \times 0.5 \quad (10.26)$$

where  $I_{dr}$  and  $I_{df}$  are the instantaneous direct and diffuse solar irradiance, respectively ( $\text{W m}^{-2} \text{ ground}$ ). Total PAR irradiance is assumed to be 50% of total solar irradiance, and  $1 \text{ W m}^{-2} \text{ ground}$  is taken as equal to  $4.55 \mu\text{mol photons m}^{-2} \text{ ground s}^{-1}$  (Goudriaan and van Laar, 1994).

The reflection coefficients  $p_{dr}$  and  $p_{df}$  are determined from Goudriaan (1977) by

$$p_{dr} = \text{MAX} \llbracket 0.04, p_s \exp(-2k_{dr}\omega\sqrt{0.8}L) \rrbracket \quad (10.27)$$

$$p_{df} = \text{MAX} \llbracket 0.04, p_s \exp(-2k_{df}\sqrt{0.8}L) \rrbracket \quad (10.28)$$

where  $p_s$  is the soil reflection coefficient, taken as 0.15.

Assuming the oil palm canopies are randomly distributed in the aerial space, the canopy extinction coefficient for direct PAR  $k_{dr}$  is determined by

$$k_{dr} = 0.5/\cos\theta \quad (10.29)$$

where  $\theta$  is the solar inclination (radians). Eq. 10.29, however, is valid only fully closed canopies. For discontinuous or partially closed canopies,  $k_{dr}$  must be multiplied by a clump factor  $\omega$  which ranges from 0 (no canopy) to 1 (fully closed canopies), and which can be determined by Kustas and Norman (1999) as

$$\omega = \omega_0 + 6.6557(1 - \omega_0)\exp[\exp(-\theta + 2.2103)] \quad (10.30a)$$

$$\omega_0 = \frac{1}{k_{dr}L} \ln \left\{ \tau_b + (1 - \tau_b)\exp \left[ -k_{dr} \frac{L}{1 - \tau_b} \right] \right\} \quad (10.30b)$$

where  $\omega_0$  is the canopy clustering coefficient when the sun is at zenith (highest point in the sky); and  $\tau_b$  is the canopy gap fraction (0 to 1). Awal (2008) measured the canopy gap fraction for various oil palm tree ages, and reanalyzing and fitting the best function to his measured data,  $\tau_b$  can be estimated from  $L$  by

$$\tau_b = (1 + 1.33\sqrt{L})^{-1} \quad (10.31)$$

Following the method by Teh (2006), the canopy extinction coefficient for diffuse PAR  $k_{df}$  is determined by integrating the light penetration function based on Beer's law (together with Eq. 10.29 to 10.31) over the whole sky (assuming a uniform bright sky) and for several leaf area indexes  $L$  to finally obtain the following estimate of  $k_{df}$ :

$$k_{df} = \exp(0.038042 - 0.38845\sqrt{L}) \quad (10.32)$$

Note that this  $k_{df}$  estimation already accounts for discontinuous canopies by the use of Eq. 10.30 in the integration.

The PAR flux densities absorbed by the oil palm canopies is distinguished into two components: that absorbed by the canopies directly exposed to direct PAR (sunlit portion of  $L$ ) and that absorbed by the portion of canopies shaded from direct PAR (shaded  $L$ ). Dividing the oil palm canopies in this way, rather than treating the canopies as one whole, would provide a more accurate estimation of canopy photosynthesis because the CO<sub>2</sub> assimilation by the sunlit and shaded portions of the canopies would often be different from each other.

$L_{sl}$  and  $L_{sh}$  are sunlit and shaded leaf area index, respectively (both in  $\text{m}^2$  leaf  $\text{m}^{-2}$  ground), and they can be estimated by Goudriaan and van Laar (1994) as

$$L_{sl} = \frac{1 - \exp(-k_{dr}\omega L)}{k_{dr}\omega} \quad (10.33)$$

$$L_{sh} = L - L_{sl} \quad (10.34)$$

$Q_{sl}$  and  $Q_{sh}$  are the PAR flux densities absorbed by the sunlit leaves and shaded leaves, respectively (both in  $\mu\text{mol photons m}^{-2}$  leaf  $\text{s}^{-1}$ ), and they can be determined by Campbell and Norman (1998) as

$$Q_{sl} = 0.8(k_{dr}\omega Q_{dr} + \overline{Q_{p,df}} + Q_{p,dr,\alpha}) \quad (10.35)$$

$$Q_{sh} = 0.8(\overline{Q_{p,df}} + Q_{p,dr,\alpha}) \quad (10.36)$$

Note that the PAR flux densities absorbed ( $Q_{sl}$  and  $Q_{sh}$ ) are on a per unit leaf area (not per unit ground area).

### 2.2.3 Sink-limited assimilation ( $v_s$ )

Besides limitations by Rubisco and light, photosynthesis could also be limited by the amount of sink in the oil palm, where the greater the storage or sink, the slower the photosynthetic rate, akin to chemical reactions which slow down due to the buildup of products. In a plant, the most likely limiting sink is the storage of sucrose, and Collatz et al. (1991) assumed that  $v_s$  is merely half of the maximum Rubisco capacity rate:

$$v_s = 0.5V_{cmax} \quad (10.37)$$

## 2.3 Energy balance

The energy balance of the soil-plant-atmosphere system is described as a network of resistances in which latent and sensible heat fluxes must traverse within the system to reach some reference level above the canopies (Fig. 10.4) (Shuttleworth and Wallace, 1985). Solving the energy balance gives the potential water loss by soil evaporation and plant transpiration.

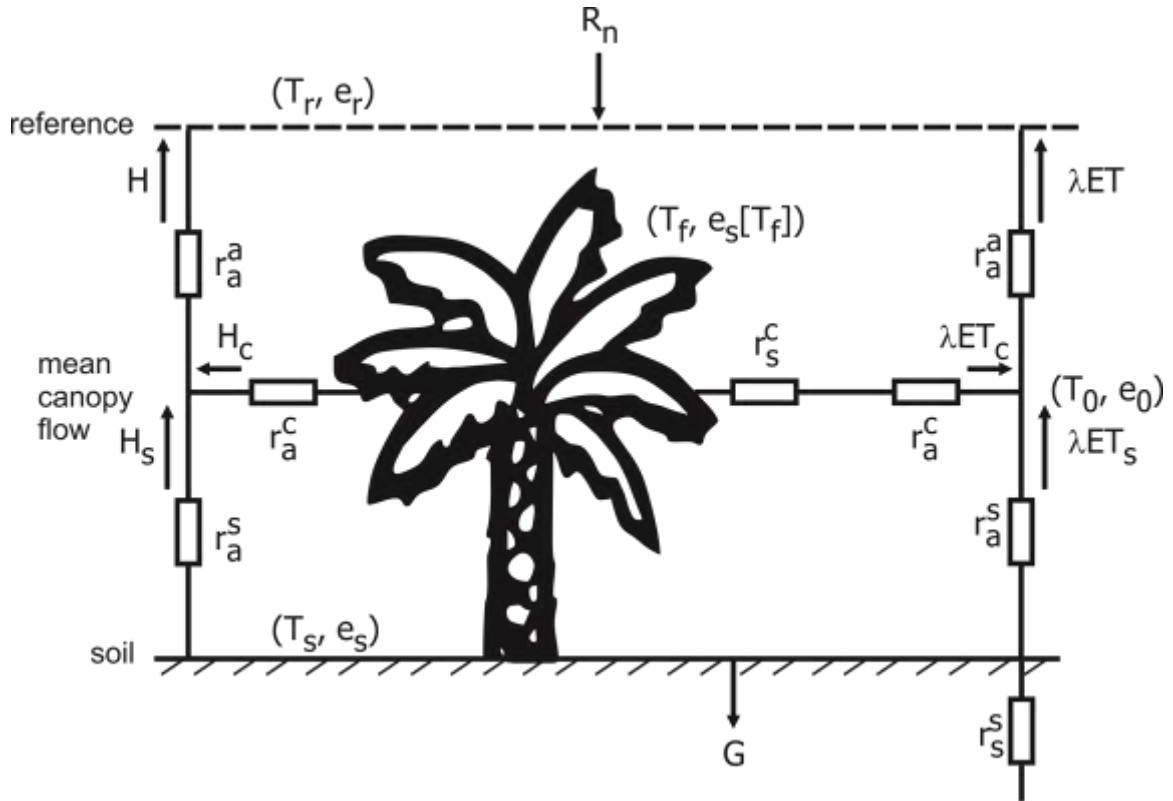


Fig. 10.4 Energy balance of the oil palm system described as a network of resistances. Key:  $\lambda ET$  and  $H$  are components of the latent and sensible heat fluxes, respectively;  $R_n$  is the net radiation flux;  $G$  is the heat flux into the soil;  $T$  and  $e$  are the temperature and vapor pressure components;  $e_s[T]$  is saturated vapour pressure at temperature  $T$ ;  $r_a^a$  and  $r_a^s$  are the aerodynamic resistances; and  $r_a^c$ ,  $r_s^c$ , and  $r_s^s$  are the surface resistances.

The energy balance in Fig. 10.4 can be described in eight independent equations, and as shown by Teh (2006) and Shuttleworth and Wallace (1985), these equations can be solved and summarized by the following series of equations to determine the total latent heat flux:

$$\lambda ET = C_c PM_c + C_s PM_s \quad (10.38a)$$

$$PM_c = \frac{\Delta A + (\rho c_p D - \Delta r_a^c A_s) / (r_a^a + r_a^c)}{\Delta + \gamma [1 + r_s^c / (r_a^a + r_a^c)]} \quad (10.38b)$$

$$PM_s = \frac{\Delta A + (\rho c_p D - \Delta r_a^s A_c) / (r_a^a + r_a^s)}{\Delta + \gamma [1 + r_s^s / (r_a^a + r_a^s)]} \quad (10.38c)$$

$$C_c = \{1 + R_c R_a / [R_s (R_c + R_a)]\}^{-1} \quad (10.38d)$$

$$C_s = \{1 + R_s R_a / [R_c (R_s + R_a)]\}^{-1} \quad (10.38e)$$

$$R_a = (\Delta + \gamma) r_a^a \quad (10.38f)$$

$$R_c = (\Delta + \gamma) r_a^c + \gamma r_s^c \quad (10.38g)$$

$$R_s = (\Delta + \gamma) r_a^s + \gamma r_s^s \quad (10.38h)$$

where  $\lambda ET$  is the total latent heat flux ( $W m^{-2}$ );  $r_a^a$  is the aerodynamic resistance between the mean canopy flow and reference height ( $s m^{-1}$ );  $r_a^s$  is the aerodynamic resistance between the soil and mean canopy flow ( $s m^{-1}$ );  $r_a^c$  is the bulk boundary layer resistance ( $s m^{-1}$ );  $r_s^c$  and  $r_s^s$  are the canopy and soil surface resistance, respectively (both in  $s m^{-1}$ );  $A$ ,  $A_s$ , and  $A_c$  are energy available to the system (total), soil, and crop, respectively (all in  $W m^{-2}$ );  $\Delta$  is the slope of the saturated vapor pressure curve ( $mbar K^{-1}$ );  $\gamma$  is the psychrometric constant ( $0.658 mbar K^{-1}$ );  $D$  is the air vapor pressure deficit ( $mbar$ ); and  $\rho c_p$  is the volumetric heat capacity for air ( $1221.09 J m^{-3} K^{-1}$ ).

Determination of total latent heat flux  $\lambda ET$  allows the determination of the vapor pressure deficit  $D_0$  ( $mbar$ ) at the theoretical mean canopy flow height as

$$D_0 = D + \frac{r_a^a}{\rho c_p} [\Delta A - (\Delta + \gamma) \lambda ET] \quad (10.39)$$

so that  $D_0$  can in turn be used to determine the partitioning of the total latent heat flux  $\lambda ET$  and total sensible heat flux  $H$  into their respective soil ( $\lambda ET_s$  and  $H_s$ ) and crop ( $\lambda ET_c$  and  $H_c$ ) flux components:

$$\lambda ET_s = \frac{\Delta A_s + \rho c_p D_0 / r_a^s}{\Delta + \gamma (r_s^s + r_a^s) / r_a^s} \quad (10.40)$$

$$\lambda ET_c = \frac{\Delta A_c + \rho c_p D_0 / r_a^c}{\Delta + \gamma (r_s^c + r_a^c) / r_a^c} \quad (10.41)$$

$$H_s = \frac{\gamma A_s (r_s^s + r_a^s) - \rho c_p D_0}{\Delta r_a^s + \gamma (r_s^s + r_a^s)} \quad (10.42)$$

$$H_c = \frac{\gamma A_c (r_s^c + r_a^c) - \rho c_p D_0}{\Delta r_a^c + \gamma (r_s^c + r_a^c)} \quad (10.43)$$

where all the soil and crop heat flux components are in  $W m^{-2}$ .

Numerical Gaussian integration method is used to obtain the daily latent heat and sensible fluxes (Teh, 2006). This is so that the daily amount of water transpired (by plants) and evaporated (by soil) can be known. Five points over 24 hours in a day are selected, and for each selected hour, the heat fluxes are calculated.

### 2.3.1 Available energy

The balance of net radiation  $R_n$  after soil heat flux  $G$  is the energy available to the crop  $A_c$  and soil  $A_s$  (all in  $W m^{-2}$ ), or

$$A = A_s + A_c = R_n - G \quad (10.44a)$$

$$A_s = R_n \tau_{dr,\alpha} - G \quad (10.44b)$$

$$A_c = R_n (1 - \tau_{dr,\alpha}) \quad (10.44c)$$

$$G = R_n [t_c + \tau_{dr,\alpha} (t_s - t_c)] \quad (10.44d)$$

$$\tau_{dr,\alpha} = \exp(-k_{dr} \omega \sqrt{0.5L}) \quad (10.44e)$$

where  $L$  is the total leaf area index ( $m^2$  leaf  $m^{-2}$  ground);  $k_{dr}$  is the canopy extinction coefficient for direct solar radiation;  $\omega$  is the canopy clustering coefficient; and  $t_c$  and  $t_s$  are the fraction of net radiation as soil heat flux under full canopies and for bare soil (no canopies), respectively. Parameters  $t_c$  and  $t_s$  are taken as 0.05 (Monteith, 1973) and 0.315 (Kustas and Daughtry, 1990), respectively.

Following Brutsaert (1982), net radiation  $R_n$  ( $W m^{-2}$ ) is determined as the difference between the incoming shortwave radiation  $I_t$  ( $W m^{-2}$ ) and outgoing net longwave radiation  $R_{nL}$  ( $W m^{-2}$ ):

$$R_n = (1 - p)I_t + R_{nL} \quad (10.45a)$$

$$R_{nL} = 0.98\sigma(T_a + 273.15)^4 \left[ 1.31 \left( \frac{e_a}{T_a + 273.15} \right)^{1/7} - 1 \right] \quad (10.45b)$$

where  $p$  is the surface albedo (0.15); and  $\sigma$  as the Stefan-Boltzmann constant ( $5.67 \times 10^{-8} \text{ W m}^{-2} \text{ K}^{-4}$ ).

### 2.3.2 Vertical profile of wind speed and eddy diffusivity

Wind speed decreases exponentially with decreasing height due to increasing drag until wind speed theoretically reaches zero at a height equal to the total height of zero plane displacement  $d$  and crop roughness length  $z_0$ . The methods by Su et al. (2001) and Massman (1997) are adapted to determine  $d$  and  $z_0$  (both in m) as

$$d = h\Delta H \quad (10.46a)$$

$$z_0 = h(1 - \Delta H)\exp(-k/0.32) \quad (10.46b)$$

$$\Delta H = 1 - \frac{\exp(-2k_w)[\exp(-2k_w) - 1]}{2k_w} \quad \text{for } 0.30 \leq \Delta H \leq 0.95 \quad (10.46c)$$

where  $k_w$  is the vertical wind speed extinction coefficient (unitless);  $h$  is the tree height (m); and  $k$  is the von Karman constant (0.4).

Vertical wind speed extinction coefficient  $k_w$  (assumed equal to eddy diffusivity  $k_e$ ) increases with increasing leaf area index. Simulations by Massman (1987) for hypothetical canopies with uniform foliage density were used by Nikolov and Zeller (2003) to approximate the relationship between  $k_w$  and total leaf area index  $L$  ( $\text{m}^2 \text{ leaf m}^{-2} \text{ ground}$ ) simply as

$$k_w = k_e = 3[1 - \exp(-L)] \quad (10.47)$$

The wind speed at the canopy height  $u_h$  ( $\text{m s}^{-1}$ ) is determined by

$$u_h = \frac{u_*}{k} \ln\left(\frac{h-d}{z_0}\right) \quad (10.48)$$

where  $u_*$  is the friction velocity ( $\text{m s}^{-1}$ ), determined by

$$u_* = \frac{ku}{\ln\left(\frac{z_r-d}{z_0}\right)} \quad (10.49)$$

where  $u$  is the wind speed ( $\text{m s}^{-1}$ ) measured at the reference height  $z_r$  (m).

### 2.3.3 Resistances

Aerodynamic resistances are calculated by

$$r_a^s = \frac{\exp(k_e)}{k_e k u_*} \left[ \exp\left(-k_e \frac{z_{s0}}{h}\right) - \exp\left(-k_e \frac{z_0 + d}{h}\right) \right] \quad (10.50)$$

$$r_a^a = \frac{1}{k_e u_*} \ln\left(\frac{z_r - d}{h - d}\right) + \frac{1}{k_e k u_*} \left\{ \exp\left[k_e \left(1 - \frac{z_0 + d}{h}\right)\right] - 1 \right\} \quad (10.51)$$

where  $r_a^s$  and  $r_a^a$  are the aerodynamic resistance between the mean canopy flow and reference height and between the soil and mean canopy flow, respectively (both in  $s\ m^{-1}$ ); and  $z_{s0}$  is the soil surface roughness length (m), taken as 0.004, the value for a flat, tilled land (Hansen, 1993).

Calculations are adapted from Campbell and Norman (1998) to determine the bulk boundary layer resistance  $r_a^c$  ( $s\ m^{-1}$ ) as

$$r_a^c = \frac{k_w}{0.01 L_{eff} [1 - \exp(-0.5 k_w)] \sqrt{u_h/w}} \quad (10.52)$$

where  $L_{eff}$  is the effective leaf area index ( $m^2\ leaf\ m^{-2}\ ground$ ); and  $w$  is the mean leaf width (m), which, for oil palm pinnae, can be determined from Rao et al. (1992) as

$$w = 0.0165 + 0.0152 \ln(age/365) \quad (10.53)$$

where  $age$  is the tree age (days).

Not all leaves, especially at near or full canopy, would contribute equally to affect fluxes. This is due to self-shading of leaves. Consequently, Szeicz and Long (1969) recommended that an effective leaf area index  $L_{eff}$  be used instead of total  $L$ , where  $L_{eff}$  is taken as the smaller between the current leaf area index  $L$  or half of the maximum possible leaf area index; that is,

$$L_{eff} = \text{MIN} \left[ L, 0.5 L_{max,PD} \right] \quad (10.54)$$

where  $L_{max,PD}$  is the maximum leaf area index ( $m^2\ leaf\ m^{-2}\ ground$ ) for a given  $PD$  planting density (palms  $ha^{-1}$ ), and for oil palm,  $L_{max,PD}$  is determined by

$$L_{max,PD} = 0.0274PD^{1/A} \quad (10.55)$$

where  $A$  is 0.935. Eq. 10.55 was derived by fitting the best function to the maximum  $L$  obtained in various oil palm planting densities from Foong (1999), Kwan (1994), Rao et al. (1992), and Tan and Ng (1977).

Canopy resistance is determined by scaling up leaf stomatal resistance (the inverse of leaf stomatal conductance) to the canopy level by

$$r_s^c = 1/(gst \times L_{eff}) \quad (10.56)$$

where  $r_s^c$  is the canopy resistance ( $s \text{ m}^{-1}$ ); and  $gst$  is the leaf stomatal conductance ( $\text{m s}^{-1}$ ).

Leaf stomatal conductance  $gst$  is at maximum conductance  $gst_{max}$ , but water stress, low PAR irradiance, and vapor pressure deficit will reduce  $gst$  by the following relationships:

$$gst = gst_{max} \times f_{water} \times f_{PAR} \times f_D \quad (10.57a)$$

$$f_{water} = ET_c/PET_c \quad (10.57b)$$

$$f_{PAR} = gst_{PAR}[[PAR]]/gst_{PAR}[[PAR_{max}]] \quad (10.57c)$$

$$gst_{PAR}[[PAR]] = 0.014614[1 - \exp(-0.008740PAR)] \quad (10.57d)$$

$$f_D = gst_D[[D]]/gst_D[[D_{min}]] \quad (10.57e)$$

$$gst_D[[D]] = 0.031970 - 0.007516\ln(D) \quad (10.57f)$$

where  $gst_{max}$  for oil palm is  $500 \text{ mmol H}_2\text{O m}^{-2} \text{ leaf s}^{-1}$  or  $0.0125 \text{ m s}^{-1}$  (Kallarackal et al., 2004); and  $f_{PAR}$ ,  $f_{water}$ , and  $f_D$  are scaled reductions from 0 to 1 to  $gst_{max}$  due to PAR irradiance, water stress, and vapor pressure deficit, respectively.

Note that crop water stress is described in Eq. 10.57b, where the level of stress is determined, following Kropff (1993), as the ratio between the actual and potential transpiration ( $ET_c$  and  $PET_c$ , respectively; both in  $\text{m day}^{-1}$ ).

Eq. 10.57d and 10.57f were derived by fitting the best functions to measured leaf stomatal conductance at several levels of PAR and air vapor pressure deficit  $D$  (Fig. 10.5). Leaf stomatal conductance for palm ages 1 to 20 yrs were measured using the AP4 dynamic

diffusion porometer (Delta-T Devices Ltd., Cambridge, UK). From Fig. 10.5a,  $PAR_{max}$ , which is the maximum PAR irradiance ( $W m^{-2}$ ) for maximum leaf conductance, is taken at  $330 W m^{-2}$  (or  $1500 \mu mol photons m^{-2} ground s^{-1}$ ) (Dufrêne and Saugier, 1993). Similarly, maximum conductance occurs when air vapor pressure deficit is minimum ( $D_{min}$ ), taken at 10 mbar (Fig. 10.5b).

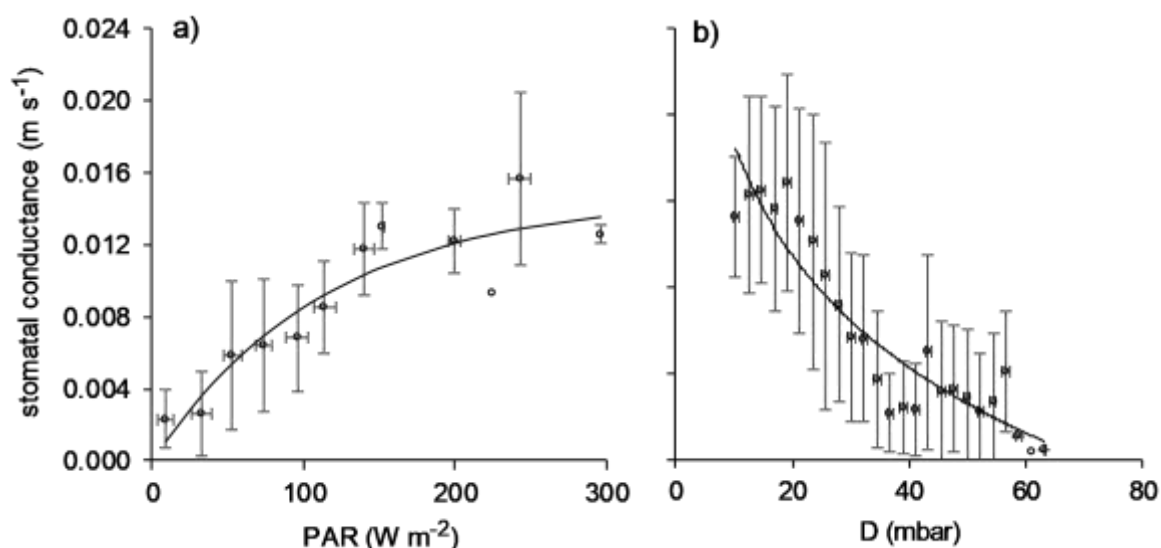


Fig. 10.5 Relationship between measured leaf stomatal conductance with: a) photosynthetically active radiation (PAR) irradiance ( $N = 381$ ), and b) air vapor pressure deficit  $D$  ( $N = 2591$ ). Leaf measurements were on 1- to 20-yr oil palm trees. Note: the bars represent one standard deviation.

Finally, soil surface resistance  $r_s^s$  ( $s m^{-1}$ ) is determined solely from the first (topmost) soil layer as this is the layer in direct contact with the atmosphere. Equations from Farahani and Ahuja (1996) and Choudhury and Monteith (1988) are followed:

$$r_s^s = \frac{\tau l}{\phi_p D_{m,v}} \exp\left(-\frac{1}{\lambda} \times \frac{\theta}{\theta_0}\right) \quad (10.58)$$

where  $D_{m,v}$  is the vapor diffusion coefficient in air ( $24.7 \times 10^{-6} m^2 s^{-1}$ );  $\phi_p$  is the soil porosity ( $m^3 m^{-3}$ );  $l$  is the soil layer thickness of the first soil layer (m);  $\theta$  is the volumetric soil water content ( $m^3 m^{-3}$ );  $\theta_0$  is the saturated soil water content ( $m^3 m^{-3}$ );  $\lambda$  is the soil pore-size distribution index or the slope of the logarithmic suction-soil moisture curve (Bittelli et al., 2015); and  $\tau$  is the soil tortuosity (unitless), determined from Shen and Chen (2007) as

$$\tau = \sqrt{\phi_p + 3.79(1 - \phi_p)} \quad (10.59)$$

Soil properties and water flow in oil palm plantations are discussed next.

## 2.4 Soil water

Rather than treating the whole soil profile as one large and homogenous soil layer, it is more accurate to divide the soil profile into two or more soil layers and then use Darcy's law to describe the flow of water from one soil layer to the next, taking into account the physical properties of each soil layer (Fig. 10.6). Water flow is modeled following the 'tipping bucket' system, where water flow is treated in a sequential manner, beginning in the first soil layer, then moving successively down through the soil profile until to the last soil layer.

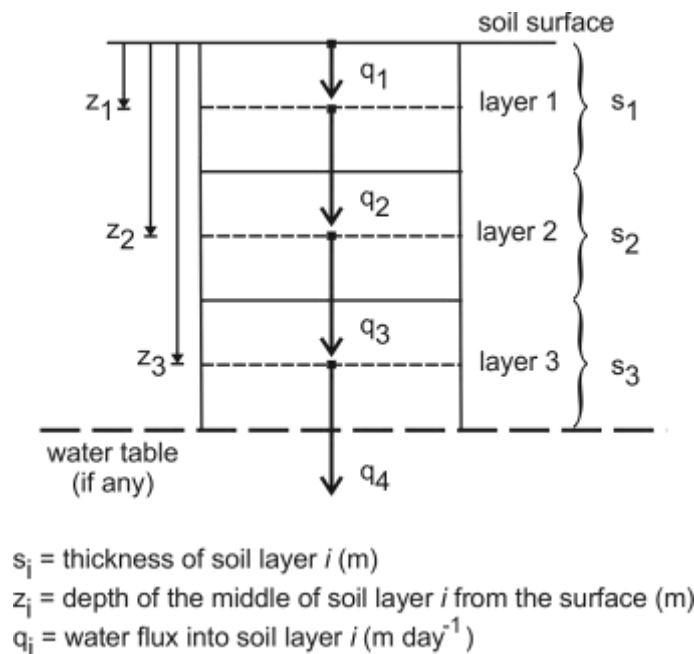


Fig. 10.6. Water flow in a soil profile is divided into three successive layers, with the presence of a water table, if any, always just beneath the last (in this case, third) soil layer.

It is recommended to divide a soil profile into two or more consecutive layers, with first soil layer as a thin layer, and the second layer covering up to at least the entire rooting depth. Soil layer  $i$  ( $i = 1$  to  $M$ ) has a thickness of  $s_i$  (m), and the depth from the soil surface to the middle of layer  $i$  is  $z_i$ .

Water flux into soil layer  $i$  is denoted as  $q_i$  ( $\text{m day}^{-1}$ ). Water flow follows the downward positive coordinate system, where the downward and upward direction of flow of water are taken as a positive and negative value, respectively, and the reference level is taken as the soil surface

level. Darcy's law is used to describe the water flow in the soil. Water flow is taken to occur from the middle of layer  $i - 1$  to the middle of layer  $i$ . The method based on Campbell (1994) is followed. Water flux into soil layer  $i$  is:

$$q_i = \begin{cases} P_{net} - ET_s - ET_{c,i} & i = 1 \\ \overline{K_{\theta,i}} \frac{H_i - H_{i-1}}{z_i - z_{i-1}} - ET_{c,i} & 1 < i \leq N \\ K_{\theta,N} & i = N + 1 \end{cases} \quad (10.60a)$$

$$\overline{K_{\theta,i}} = \frac{K_{\theta,i-1} - K_{\theta,i}}{\ln K_{\theta,i-1} - \ln K_{\theta,i}} \quad (10.60b)$$

where  $q$  is the water flux ( $\text{m day}^{-1}$ );  $P_{net}$  is the net daily rainfall ( $\text{m day}^{-1}$ );  $ET_s$  is the actual daily soil evaporation (occurs only from the first soil layer) ( $\text{m day}^{-1}$ );  $ET_c$  is the daily extraction of water by roots (actual plant transpiration) ( $\text{m day}^{-1}$ );  $\overline{K_{\theta,i}}$  is the logarithmic mean of the hydraulic conductivities of layer  $i$  and  $i - 1$  ( $\text{m day}^{-1}$ );  $z$  is the soil layer's depth (m); and  $H$  is the total head (matric suction and gravity heads) (m). Note that water table, if present, is treated as an additional but saturated soil layer  $N+1$ , and Eq. 10.60 used to describe the capillary rise of water.

Water flux out of the last soil layer ( $i = M$ ) is denoted by  $q_{N+1}$ , and without the presence of a water table, it is merely equal to  $K_{\theta,N}$  because it is assumed that the soil below the last layer is uniformly wet and it has the same water content as the last soil layer. Consequently, water flux is only due to gravity gradient (no matric suction gradient). In this case,  $q_{N+1} = K_{\theta,N}$ .

The net flux  $\hat{q}_i$  ( $\text{m day}^{-1}$ ) in soil layer  $i$  is the difference between incoming  $q_i$  and outgoing water  $q_{i+1}$  fluxes:

$$\hat{q}_i = q_{i-1} - q_{i+1} \quad (10.61)$$

where a positive net flux means soil water content has increased, and in contrast, a negative net flux denotes the soil is drying. This means that the change in the soil water content is determined by:

$$\Theta_{i,t+1} = \Theta_{i,t} + \hat{q}_i \quad (10.62)$$

where  $\Theta_{i,t}$  and  $\Theta_{i,t+1}$  are the water content in soil layer  $i$  (m) between two successive time steps  $t$  and  $t+1$ , respectively.

For each soil layer  $i$ , the volumetric soil water content ( $\text{m}^3 \text{m}^{-3}$ ) at permanent wilting point  $\theta_{1500}$ , field capacity  $\theta_{33}$ , and saturation  $\theta_0$  are estimated from the soil's primary particles (clay and sand) and organic matter contents based empirical equations from Saxton and Rawls (2006). Matric suction head and soil hydraulic conductivity ( $\text{m day}^{-1}$ ) for saturated  $K_{s,i}$  and unsaturated  $K_{\theta,i}$  flows are estimated based on Bittelli et al. (2015) and Saxton and Rawls (2006), using the geometric mean distribution of the soil's primary particles.

Actual soil evaporation  $ET_s$  (taken as  $\text{m day}^{-1}$ ) is calculated from Teh (2006) and van Keulen and Seligman (1987) as

$$ET_s = PET_s \times R_{Ds} \quad (10.63a)$$

$$R_{Ds} = \frac{1}{1 + (3.607\theta_1/\theta_{s,1})^{-9.3172}} \quad (10.63b)$$

where  $PET_s$  is the potential evaporation ( $\text{m day}^{-1}$ );  $R_{Ds}$  is the reduction factor for evaporation (ranging from 0 to 1); and  $\theta_1$  and  $\theta_{s,1}$  are the current and saturated soil water content, respectively, for the first soil layer ( $i = 1$ ) (both in  $\text{m}^3 \text{m}^{-3}$ ). Note: potential soil evaporation is  $\lambda ET_s$  ( $\text{W m}^{-2}$ ) from Eq. 10.40 is divided by  $\lambda$  ( $2454000 \text{ J kg}^{-1}$ ) and multiplied by 86.4 to obtain  $PET_s$  in  $\text{m day}^{-1}$ .

Actual transpiration ( $ET_c$ ,  $\text{m day}^{-1}$ ) is calculated from Kropff (1993) as

$$ET_c = PET_c \times R_{Dc} \quad (10.64a)$$

$$R_{Dc} = \begin{cases} 1 & \theta_{root} \geq \theta_{cr,root} \\ \frac{\theta_{root} - \theta_{1500,root}}{\theta_{cr,root} - \theta_{1500,root}} & \theta_{1500,root} < \theta_{root} < \theta_{cr,root} \\ 0 & \theta_{root} \leq \theta_{1500,root} \end{cases} \quad (10.64b)$$

$$\theta_{cr,root} = \theta_{1500,root} + p(\theta_{0,root} - \theta_{1500,root}) \quad (10.64c)$$

where  $PET_c$  is the potential transpiration (after converting  $\lambda ET_c$  from Eq. 10.41 into  $\text{m day}^{-1}$ );  $R_{Dc}$  is the reduction factor for transpiration (0 to 1);  $\theta_{root}$  is the soil water content currently in the root zone;  $\theta_{1500,root}$  and  $\theta_{0,root}$  are the soil root zone's permanent wilting point and

saturation, respectively; and  $\theta_{cr,root}$  is the volumetric water content in the root zone below which water stress occurs. All soil water content are in  $m^3 m^{-3}$ .

For C3 plants in general,  $p$  in Eq. 10.64c is often taken as 0.5. However, comparing the soil water content between irrigated and non-irrigated oil palm trials from 1983 to 1990 by Foong (1999) suggested that oil palm is more sensitive to water stress because  $p$  is more likely 0.6 than 0.5 of  $(\theta_{0,root} - \theta_{1500,root})$ . This 0.6 critical point corresponds to about 45% of the available soil water content (AWC) of Munchong soil series (Typic Hapludox), the type of soil in the oil palm trials by Foong (1999). Incidentally, Rey et al. (1998) also observed that oil palm stomatal conductance would begin to decline only when the soil water content fell below the level of about 50% of their soil's AWC (Fig. 10.7).

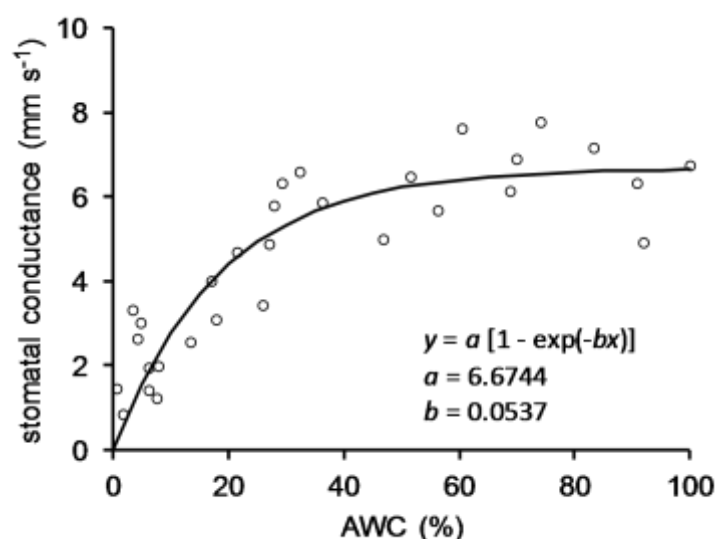


Fig. 10.7. Fitting a function to the relationship between oil palm leaf stomatal conductance and available soil water content (AWC), as measured by Rey et al. (1998). Stomatal conductance declined only when AWC was about 50% or less.

The amount of water extracted by roots in each soil layer is based on the measured data for oil palm by Nelson et al. (2006) and on the root water uptake algorithm by Miyazaki (2005):

$$ET_{c,i} = ET_c(\varphi_i - \varphi_{i-1}) \quad (10.65a)$$

$$\varphi_i = 1.8c_j - 0.8c_j^2 \quad (10.65b)$$

$$c_j = \text{MIN}[[1, S_j/d_{root}]] \quad (10.65c)$$

where  $S_j$  is the cumulative thickness of soil layer  $j$  (summation of thickness of the current soil layer and all its preceding soil layers ).

Lastly, net rainfall  $P_{net}$  refers to the amount of rain reaching the ground as both throughfall and stemflow. The larger the canopy cover or leaf area index, the larger the fraction of intercepted gross rainfall by the canopies and the smaller the net rainfall. Net rainfall studies on closed oil palm canopies by Lubis (2016), Chong (2012), Bentley (2007), Zulkifli et al. (2006), and Damih (1995) showed that throughfall and stemflow are on average ( $\pm$  s.e.)  $61.3 \pm 2.1$  and  $8.4 \pm 1.0\%$  of  $P_g$ , respectively (N = 430 rain events).  $P_{net}$  ( $m \text{ day}^{-1}$ ) is related to oil palm leaf area index  $L$  ( $m^2 \text{ leaf } m^{-2} \text{ ground}$ ) and  $P_g$  ( $m \text{ day}^{-1}$ ) as follows:

$$P_{net} = P_g \times \text{MAX}[[0.7295, 1 - 0.0541L]] \quad (10.66)$$

where it is assumed that  $P_{net}/P_g$  decreases linearly with  $L$  until closed canopies are reached, after which  $P_{net}$  never exceeds 72.95% of  $P_g$  (Fig. 10.8).

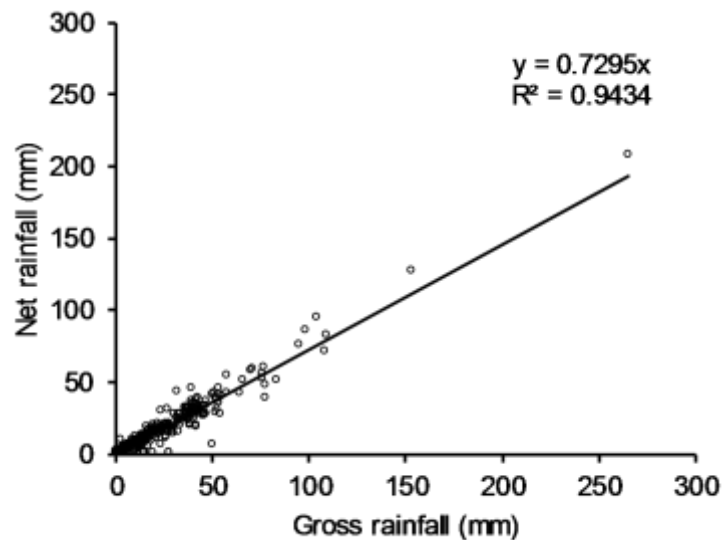


Fig. 10.8. Strong linear relationship between net rainfall and gross rainfall under closed oil palm canopies (Lubis, 2016; Chong, 2012; Bentley, 2007; Zulkifli et al., 2006; Damih, 1995) (N = 430).

Fig. 10.9 shows the accuracy of this soil water model component when it was tested against field measurements of soil water content at several soil depths (0.15 to 0.90 m) under fully matured oil palms (20 yrs old;  $148 \text{ palms } ha^{-1}$ ) at an oil palm estate at Serdang, Malaysia ( $2.98053403^\circ N$ ,  $101.72884214^\circ E$ ). Daily soil water measurements were for 167 days from Jul. 17, 2012. The soil type was Munchong series (Typic Hapludox), with a rather homogenous

soil profile (54% clay and 37% sand). The average absolute difference between soil water predictions and measurements is 0.03 mm.

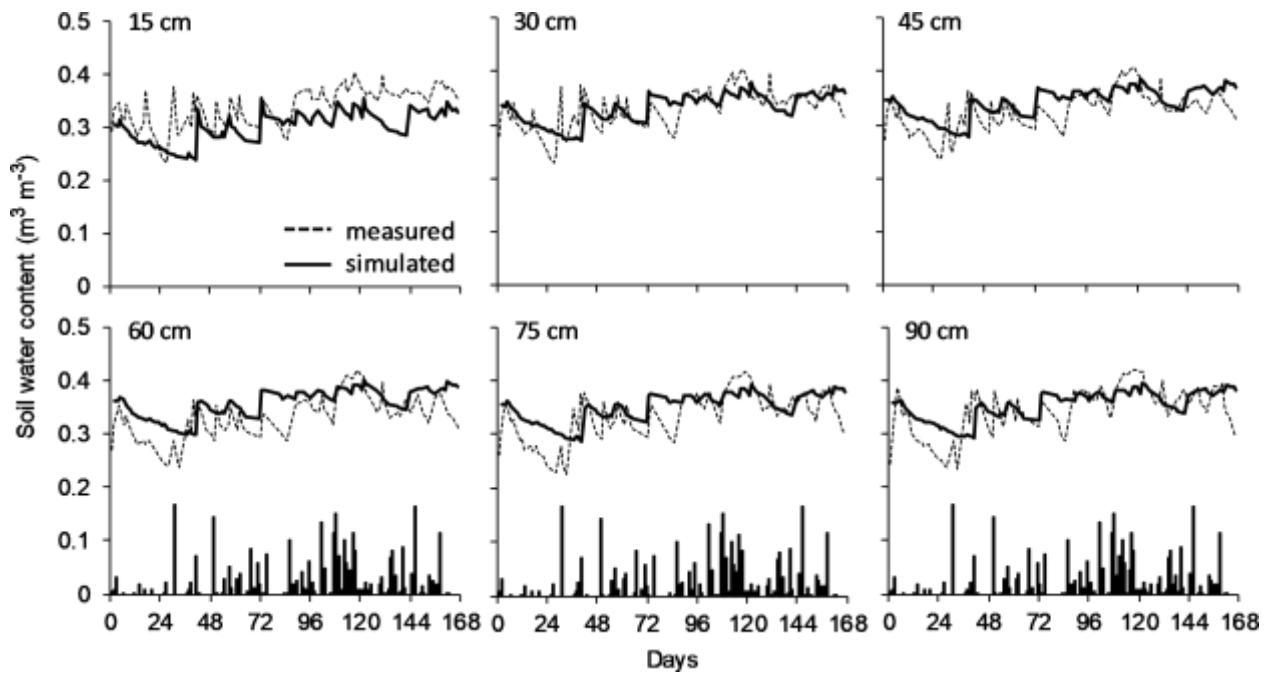


Fig. 10.9. Comparisons between simulated and measured soil water content at several soil depths (from 15 to 90 cm) under fully matured oil palms. Note the bar charts in the lower panel represent the daily rainfall amount (mm) (total rainfall during this period was 1890 mm, with a maximum daily rainfall of 100 mm).

## 2.5 Crop growth

Plant assimilates (expressed as amount of  $\text{CH}_2\text{O}$ ) produced via photosynthesis is first used for plant maintenance respiration (supporting processes for continual plant survival) and growth respiration (synthesis of new cells) (Thornley, 1970), after which the balance is then used for generative growth (development of flowers, bunches, and yield). The method by van Kraalingen et al. (1989) for oil palm is adapted.

### 2.5.1 Maintenance respiration

The maintenance respiration for pinnae  $M_{pinnae}$ , rachis  $M_{rachis}$ , trunk  $M_{trunk}$ , and roots  $M_{roots}$  (all in  $\text{kg CH}_2\text{O palm}^{-1} \text{ day}^{-1}$ ) are as follows:

$$M_{pinnae} = W_{pinnae} \times M_{c,pinnae} \times (24 - DL)/24 \quad (10.67a)$$

$$M_{c,pinnae} = (N_{pinnae} \times 0.036 \times 6.25) + (X_{pinnae} \times 0.072 \times X_c) \quad (10.67b)$$

$$M_{rachis} = W_{pinnae} \times M_{c,rachis} \quad (10.68a)$$

$$M_{c,rachis} = (N_{rachis} \times 0.036 \times 6.25) + (X_{rachis} \times 0.072 \times X_c) \quad (10.68b)$$

$$M_{trunk} = (W_{top,trunk} + 0.06W_{bottom,trunk}) \times M_{c,trunk} \quad (10.69a)$$

$$M_{c,trunk} = (N_{trunk} \times 0.036 \times 6.25) + (X_{trunk} \times 0.072 \times X_c) \quad (10.69b)$$

$$W_{top,trunk} = \text{MIN}[[W_{trunk}, 45.0]] \quad (10.69c)$$

$$W_{bottom,trunk} = W_{trunk} - W_{top,trunk}$$

$$M_{roots} = W_{roots} \times M_{c,roots} \quad (10.70a)$$

$$M_{c,roots} = (N_{roots} \times 0.036 \times 6.25) + (X_{roots} \times 0.072 \times X_c) \quad (10.70b)$$

where  $W_{(part)}$  represents the dry weight (DM) of an individual plant part (e.g., pinnae, rachis, trunk, or roots) (kg DM palm<sup>-1</sup>);  $DL$  is the day length (hour); and  $M_{c,(part)}$  is the maintenance coefficient for a given plant part (kg CH<sub>2</sub>O kg<sup>-1</sup> DM);  $N_{(part)}$  and  $X_{(part)}$  are the nitrogen and mineral fractions (by weight) in a given plant part, respectively; and  $X_c$  is the correction factor for mineral content (unitless), taken as 2 by van Kraalingen et al. (1989).

Maintenance respiration for generative organs (bunches and flowers)  $M_{organs}$  (kg CH<sub>2</sub>O kg<sup>-1</sup> DM) is determined as follows:

$$M_{organs} = 0.0027W_{matbunch} + M_{c,rachis}(W_{immbunch} + W_{maleflo}) \quad (10.71)$$

where  $W_{matbunch}$ ,  $W_{immbunch}$ , and  $W_{maleflo}$  are the dry weights of the mature bunches, immature bunches, and male flowers, respectively (kg DM palm<sup>-1</sup>), and it is assumed that the maintenance coefficients for immature bunches and male flowers are the same as that for rachis.

Total maintenance is determined by:

$$M_{total} = M_{metabolic} + \sum_{plant\ parts} M_{(part)} \quad (10.72a)$$

$$M_{metabolic} = \frac{0.16\Lambda_{canopy,d}}{\sum_{plant\ parts} W_{(part)}} \quad (10.72b)$$

where  $M_{total}$  is the total maintenance requirement for the whole tree, which is the summation of the maintenance requirement for all plant parts, as well as that to support the metabolic activity  $M_{metabolic}$  (all units in kg CH<sub>2</sub>O palm<sup>-1</sup> day<sup>-1</sup>);  $\Lambda_{canopy,d}$  is the daily canopy photosynthesis (Eq. 10.12) (kg CH<sub>2</sub>O palm<sup>-1</sup> day<sup>-1</sup>); and  $\sum_{plant\ parts} W_{(part)}$  is the total dry weight of all plant parts (kg DM palm<sup>-1</sup>).

Maintenance respiration increases with increasing air temperature, so  $M_{total}$  must be corrected for air temperature. Correction is by using Eq. 10.15 and taking the Q<sub>10</sub> coefficient as 2. Growth of oil palm is completely inhibited when air temperature is below 15 °C (Henry, 1955). The maximum air temperature for oil palm growth is taken as 45 °C, a general maximum value for most plants (Hasanuzzaman et al., 2013). Consequently, if the current air temperature is beyond oil palm's growing temperature range of 15 to 45 °C, all assimilates will solely be for maintenance respiration.

Any balance of assimilates after maintenance respiration is available for growth respiration  $G_{growth}$  (kg CH<sub>2</sub>O palm<sup>-1</sup> day<sup>-1</sup>) as:

$$G_{growth} = MAX[[0, \Lambda_{canopy,d} - M_{total}]] \quad (10.73)$$

## 2.5.2 Growth respiration

The annual vegetative dry matter requirement  $VDM$  (kg DM palm<sup>-1</sup> year<sup>-1</sup>) is determined based on leaf area index  $L$  (m<sup>2</sup> leaf m<sup>-2</sup> ground), following a rectangular hyperbola relationship, as

$$VDM = MIN[[20, (a + b/L^{1.5})^{-1}]] \quad (10.74a)$$

$$a = A/VDM_{max,PD} \quad (10.74b)$$

$$b = 0.1(1/A - 1)(PD/100)^{1/A} \quad (10.74c)$$

$$VDM_{max,PD} = 231PD^{1-1/A} \quad (10.74d)$$

where  $VDM_{max,PD}$  is the maximum VDM for the given planting density  $PD$  (palms ha<sup>-1</sup>); and  $A$  is 0.935. Coefficients  $a$ ,  $b$ , and  $A$ , as well as  $VDM_{max,PD}$ , were obtained from fitting the best functions to measured data from van Kraalingen et al. (1989).

The growth rates  $G_{growth,(part)}$  (kg DM palm<sup>-1</sup> day<sup>-1</sup>) for the individual plant parts (pinnae, rachis, trunk, and roots) are determined by

$$G_{growth,(part)} = DM_{(part)} \times A_{growth} \times CVF \quad (10.75a)$$

$$A_{growth} = MIN \left[ \left[ \frac{VDM/365}{CVF}, G_{growth} \right] \right] \quad (10.75b)$$

$$CVF = 0.70(DM_{pinnae} + DM_{rachis}) + 0.66DM_{trunk} + 0.65DM_{roots} \quad (10.75c)$$

where  $A_{growth}$  is the actual amount of assimilates available for growth respiration (kg CH<sub>2</sub>O palm<sup>-1</sup> day<sup>-1</sup>);  $CVF$  is a factor (kg DM kg<sup>-1</sup> CH<sub>2</sub>O) to convert a weight expressed on a CH<sub>2</sub>O per weight basis to that on per dry matter (DM) basis. Dry matter partitioning  $DM_{(part)}$  for pinnae, rachis, trunk, and roots are 0.24, 0.46, 0.14, and 0.16, respectively (their mean values are from Henson and Mohd Tayeb, 2003; Henson, 1995; Corley et al., 1971).

The death rates (kg DM palm<sup>-1</sup> day<sup>-1</sup>) for leaves (pinnae and rachis) and roots are calculated based on Dr. Ian E. Henson (then at Malaysian Palm Oil Board; personal communication) as

$$G_{death,leaves} = 0.0016W_{leaves} \begin{cases} 0 & age \leq 600 \\ \frac{age - 600}{2500 - 600} & 600 < age \leq 2500 \\ 1 & age > 2500 \end{cases} \quad (10.76)$$

$$G_{death,roots} = \frac{W_{roots}}{365} \times \begin{cases} 0 & age \leq 1200 \\ 0.0000959210^{-5}age - 0.115 & 1200 < age \leq 3285 \\ 0.2 & age > 3285 \end{cases} \quad (10.77)$$

where  $age$  is the tree age (days); and  $W_{leaves}$  and  $W_{roots}$  are the dry weights of leaves and roots, respectively (both in kg DM palm<sup>-1</sup>).

The net increase in dry weight of a plant part is the difference between its growth and death rates between two successive time steps  $t$  and  $t+1$ :

$$W_{(part),t+1} = W_{(part),t} + G_{growth,(part)} - G_{death,(part)} \quad (10.78)$$

where  $W_{(part)}$  is the dry weight of a given plant part (kg DM palm<sup>-1</sup>). Note that there is no death rate for trunk:  $G_{death,trunk} = 0$ .

Leaf area index  $L$  (m<sup>2</sup> leaf m<sup>-2</sup> ground) is determined from planting density  $PD$  and the pinnae's dry weight  $W_{pinnae}$  and specific leaf area  $SLA$  (m<sup>2</sup> leaf kg<sup>-1</sup> DM):

$$L = W_{pinnae} \times SLA \times PD / 10000 \quad (10.79)$$

Any balance of assimilates after growth respiration is available for generative growth  $G_{gen}$  (kg CH<sub>2</sub>O palm<sup>-1</sup> day<sup>-1</sup>) as:

$$G_{gen} = \text{MAX}[[0, G_{growth} - A_{growth}]] \quad (10.80)$$

### 2.5.3 Generative organ growth

The so-called 'boxcar train' technique by van Kraalingen et al. (1989) is used to track the growth progress of generative organs: the male flowers, immature bunches (female flowers), and mature bunches (Fig. 10.10). Each train (one for each generative organ) comprises several boxcars whereby each boxcar represents an age class. The life span of both male flowers and immature bunches are taken as 210 days (beginning from the time when sex spikelet is first visible), and 150 days before harvest for the mature bunches (Corley et al., 1995). Consequently, the boxcar train for male flowers and immature bunches consist of 210 one-day age classes and for mature bunches 150 one-day age classes.

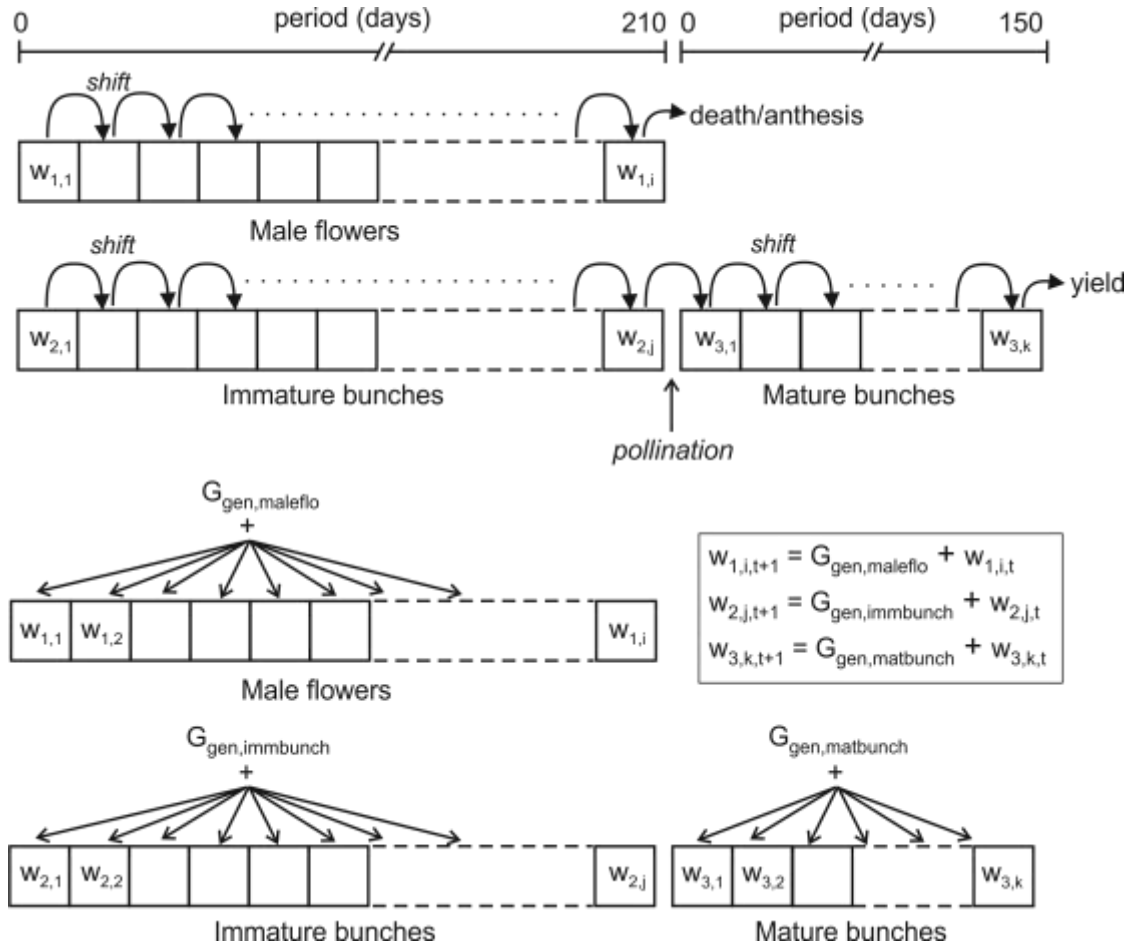


Fig. 10.10. Boxcar train schematic for growth of generative organs. In every model time step, a) weights are shifted to next age class, then b) they are incremented by the growth rate of the generative organs.

The algorithm of this boxcar train technique essentially consists of two steps: 1) the weight of a generative organ is shifted to successively older age classes, and 2) the weight is incremented according to the calculated growth rate. The lifespan of male flowers is set at 210 days, after which they will die. For the immature bunches, however, the day after 210 days marks the point of pollination, after which the growth of the pollinated bunch (*i.e.*, mature bunch) will occur. To determine the growth rates of the generative organs, the following general equations are used:

$$G_{gen,(part)} = (f_{e,(part)} \times G_{gen} \times CVF_2) / n_{(part)} \quad (10.81a)$$

$$CVF_2 = 0.70(f_{e,maleflo} + f_{e,immbunch}) + 0.44f_{e,matbunch} \quad (10.81b)$$

where  $G_{gen,(part)}$  is the growth rate for a given generative organ (male flowers, immature bunches, and mature bunches) ( $\text{kg DM day}^{-1}$ );  $G_{gen}$  is the total amount of assimilates available

for generative growth ( $\text{kg DM day}^{-1}$ );  $CVF_2$  is a factor ( $\text{kg DM kg}^{-1} \text{CH}_2\text{O}$ ) to convert dry matter weight into  $\text{CH}_2\text{O}$  weight;  $n_{(part)}$  is the number (count) of a given generative organ currently maintained; and  $f_{e,imbunch}$ ,  $f_{e,matbunch}$ , and  $f_{e,maleflo}$  are the scaled fraction of dry matter to immature bunches, mature bunches, and male flowers, respectively (all in fraction), where they are determined by

$$f_{e,(part)} = \frac{f_{(part)}}{\sum_{generative\ organs} f_{(part)}} \quad (10.82a)$$

$$f_{(part)} = DM_{(part)} \times n_{(part)} / N_{(part)} \quad (10.82b)$$

where for a given generative organ,  $DM_{(part)}$  is its share of assimilates available for generative growth (fraction) and  $N_{(part)}$  is its total growth (maturity) length (210 days for male flowers and immature bunches and 150 days for mature bunches; Fig. 10.10).  $DM_{(part)}$  for male flowers, immature bunches, and mature bunches are 0.159, 0.159, and 0.682, respectively.

In the original model of van Kraalingen et al. (1989), both male and female flowers occur in equal proportions (50:50%) and without any flower abortion. PySawit model introduces an algorithm for flower sex determination whereby if a generated random value is smaller than or equal to a preset female probability  $p_{female}$ , then the new flower is female, else male:

$$sex\ of\ new\ flower = \begin{cases} female & r \leq p_{female} \\ male & r > p_{female} \end{cases} \quad (10.83)$$

where  $p_{female}$  is the probability of having female flowers (0 to 1; 0 = no chance of female and 1 = always female); and  $r$  is a random variable uniformly distributed on [0 to 1). If  $p_{female} = 0.5$ , the tendency is to have equal proportions of male and female flowers. Consequently, the  $p_{female}$  parameter can be regarded as the genetic tendency of an oil palm planting material to produce female flowers.

Flower abortion occurs at 9 months before harvest (Corley et al., 1995), and abortion occurs if a generated random value is larger than the crop water stress level  $R_{Dc}$  (from Eq. 10.64b):

$$flower\ aborted? = \begin{cases} no & r \leq R_{Dc} \\ yes & r > R_{Dc} \end{cases} \quad (10.84)$$

Consequently, the higher the level of water stress, the smaller the value of  $R_{Dc}$ , and the greater the risk of flower abortion.

The generative organ weights are incremented between two successive time steps  $t$  and  $t+1$  simply by

$$w_{(part),i,t+1} = \begin{cases} 0 & w_{(part),i,t} = 0 \\ w_{(part),i,t} + G_{gen,(part)} & w_{(part),i,t} > 0 \end{cases} \quad (10.85)$$

where  $w_{(part),i}$  is the dry weight of a given generative organ in age class  $i$  (kg DM). The organ weights are incremented only for non-zero current weights. Thus, the total weight for a given generative organ is the summation of weights in all the age classes:

$$W_{(part)} = \sum_{i=1}^{N_{(part)}} w_{(part),i} \quad (10.86)$$

where  $N_{(part)}$  is the total maturity period for a given generative organ (days).

#### 2.5.4 Tree height and rooting depth

Measured oil palm trunk height data from Henson and Mohd Tayeb (2003), Kwan (1994), Rao et al. (1992), Breure and Powell (1988), and Jacquemard (1979, 1998) were used to develop the following equations to determine the initial trunk height  $h_{trunk(initial)}$  (m) and rate of trunk height growth  $h'_{trunk}$  (m day<sup>-1</sup>). Both are functions of tree age (days) and planting density  $PD$  (palms ha<sup>-1</sup>):

$$h_{trunk(initial)} = \exp(2.846 - 1980.888/PD^2 - 5166.366/age) \quad (10.87)$$

$$h'_{trunk} = \frac{5166.366}{0.7age^2} \times h_{trunk(initial)} \times (0.210R_{Dc} + 0.553) \quad (10.88)$$

where  $R_{Dc}$  is the crop water stress level (Eq. 10.64b).

Measurements of the canopy or crown height for oil palm trees aged between 1 to 20 yrs (N = 12) obtained the following linear regression:

$$h_{canopy} = 1.5091 + 0.001382age \quad (10.89)$$

Consequently, tree height  $h$  (m) is the summation of trunk height  $h_{trunk}$  and canopy height  $h_{canopy}$ .

Lastly, the increase in rooting depth  $d_{root}$  between two successive time steps  $t$  and  $t+1$  is

$$d_{root,t+1} = d_{root,t} + (dg_{root} \times R_{Dc}) \quad (10.90)$$

where  $dg_{root}$  is the daily increase in the rooting depth, taken as  $0.002 \text{ m day}^{-1}$ , the mean value of root growth for oil palm (Henson and Chai, 1997; Jourdan and Rey, 1997), and root growth is detrimentally affected by water stress  $R_{Dc}$  (Kropff, 1993).

## 2.6 Model testing

The accuracy of the PySawit model was evaluated by comparing its simulations with several measured growth and yield parameters of oil palm from Merlimau estate (2.253213 °N, 102.451753 °E), Melaka. The Merlimau dataset is independent and not part of the other datasets used during the development of the PySawit model.

At Merlimau, commercial *dura* x *pisifera* (AVROS x Deli Dura) palms were planted with the following planting densities: 120, 135, 148, 164, 181, 199, 220, 243, 268, and 296 palms  $\text{ha}^{-1}$ . Field plantings for all densities were simultaneously done on April 1987 when the palms were 1 yr old. At field planting, the mean ( $\pm$  s.e.) initial dry weights ( $\text{kg DM palm}^{-1}$ ) for the palm parts pinnae, rachis, trunk, and roots were  $0.40 \pm 0.07$ ,  $0.70 \pm 0.11$ ,  $0.10 \pm 0.01$ , and  $0.20 \pm 0.03$ , respectively. Field measurements continued every year until the palms were 19 yrs (Dec. 2006). Non-destructive methods by Corley and Tinker (2016), Breure (2003), Corley et al. (1971), and Hardon et al. (1969) were used to estimate leaf area and dry weights of frond (inclusive of pinnae, rachis and petiole) and trunk of oil palms. These are the oil palm industry standard methods currently being used to estimate the crop's dry matter production. At palm maturity stage, the fertilizers applied were ammonium sulfate, muriate of potash, rock phosphate, and kieserite at rates 3.5, 3.5, 2.0, and 1.25  $\text{kg palm}^{-1} \text{ yr}^{-1}$ , respectively.

The soil type at Merlimau is a sandy clay loam Rengam soil series (Typic Paleudult), and the first 0.45 m soil depth has a mean ( $\pm$  s.e.) clay, sand, organic C, and total N contents of  $27.4 \pm 0.7$ ,  $67.3 \pm 0.8$ ,  $1.7 \pm 0.1$ , and  $0.14 \pm 0.01\%$ , respectively.

PySawit required the following model inputs to be supplied: site latitude, daily weather (minimum and maximum air temperatures, wind speed, and rainfall amount), N and mineral contents in the individual plant parts of the oil palm tree, as well as the specific leaf area  $SLA$

(data obtained from van Kraalingen et al., 1989), soil properties (sand, clay, and organic matter contents), and the initial dry weights of the individual plant parts.

Three goodness-of-fit statistical indexes were used to summarize the degree of agreement between PySawit's predictions and observations. These indexes were Normalized Mean Bias Error (NMBE), Normalized Mean Absolute Error (NMAE), and the revised Willmott's index of agreement ( $d_r$ ) (Willmott et al., 2012; Yu et al., 2006). These indexes are calculated as follows:

$$NMBE = \frac{\sum_{i=1}^N P_i - O_i}{\sum_{i=1}^N O_i} \quad (10.91)$$

$$NMAE = \frac{\sum_{i=1}^N |P_i - O_i|}{\sum_{i=1}^N O_i} \quad (10.92)$$

$$d_r = \begin{cases} 1 - p/2o & p \leq 2o \\ 2o/p - 1 & p > 2o \end{cases} \quad (10.93a)$$

$$p = \sum_{i=1}^N |P_i - O_i| \quad \text{and} \quad o = \sum_{i=1}^N O_i - \bar{O} \quad (10.93b)$$

where  $P_i$  and  $O_i$  are the  $i$ -th pair of predicted and observed values, respectively ( $i = 1$  to  $N$  pairs); and  $\bar{O}$  is the mean of all observed values. NMBE (-1 to  $+\infty$ ) indicates a model's tendency to under- or overestimate relative to the mean observations. The larger the NME value, the larger the model's tendency for overestimation. NMAE (0 to  $+\infty$ ) indicates the mean absolute difference between predicted and observed values relative to the mean observations. Larger NMAE values indicate larger mean departures between model predictions and observations. The revised index of agreement  $d_r$  ranges between -1 and +1, where increasingly smaller positive or larger negative values indicate increasingly worse or inaccurate model predictions (particularly when  $d_r < 0$ ). For a perfect model, NMBE = 0 (no overall model bias), NMAE = 0, and  $d_r = +1$  (the latter two indicating perfect agreement between model predictions and observations).

### 3. Results and discussion

The mean ( $\pm$  s.e.) minimum and maximum air temperature at Merlimau from 1987 to 2006 were  $23.71 \pm 0.01$  and  $32.19 \pm 0.03$  °C, respectively. Mean daily wind speed was  $1.60 \pm 0.01$  m s<sup>-1</sup>, and the mean daily total solar irradiance was  $19.27 \pm 0.02$  MJ m<sup>-2</sup>. Mean annual rainfall was  $1918 \pm 12$  mm, with two notable dry years which occurred during 1997-98 and 2004-5

(year 11 and 18 of field planting, respectively), both of which corresponded to the occurrence of El Niño. The amount of rain received for 1997-98 and 2004-05 were 15 and 32% less than the average annual rainfall at Merlimau, respectively.

Overall, PySawit showed good agreement, with little to no bias, in predicting the growth and yield parameters of oil palm (Fig. 10.11 to 10.18). Predictions were especially good for TDM, LAI, and trunk height, as indicated by their small NMAE values ( $\leq 13\%$ ), large positive  $d_r$  values ( $>0.8$ ), and near zero NMBE values. Moreover, model accuracy remained stable across all planting densities.

However, discrepancies between yield predictions and observations increased with increasing planting density (Fig. 10.11). Yield prediction for planting density 122 palms  $\text{ha}^{-1}$  (PD122), for instance, had a high  $d_r$  value of 0.77, but this declined to 0.34 for PD296. Degree of model bias also increased with increasing planting density. Nonetheless, paired sample t-test showed no significant differences ( $p > 0.05$ ) between yield predictions and observations across all planting densities, even for PD296, although the level of significance generally declined with increasing planting density. For instance, yield predictions for PD122 was significantly different from observations only at 62% level of significance, but for PD296, this level of significance was 10%.

Both year 11 and 18 were El Niño events which caused oil palm yields to decline in year 12 (one year after the first El Niño event) and year 18 (the same year as the second El Niño event). Relative to the mean yields from yr 10 to 19, yields from all planting densities were reduced by an average ( $\pm$  s.e.) of  $12.7 \pm 4.3$  and  $11.6 \pm 4.4\%$  in year 12 and 18, respectively. Model simulations also showed a likewise decline in yields for both these years: by an average ( $\pm$  s.e.) of  $8.6 \pm 0.3\%$  in year 12 and  $18.2 \pm 0.3\%$  in year 18 (Fig. 10.11).

Simulations also revealed that at Merlimau, plant water deficit increased with increasing planting density. In PD122, the annual plant water deficit was 218 mm but in PD296, the deficit was 350 mm. Annual plant water deficit increases by average of 7 mm for every 10 palms  $\text{ha}^{-1}$  increase in planting density.

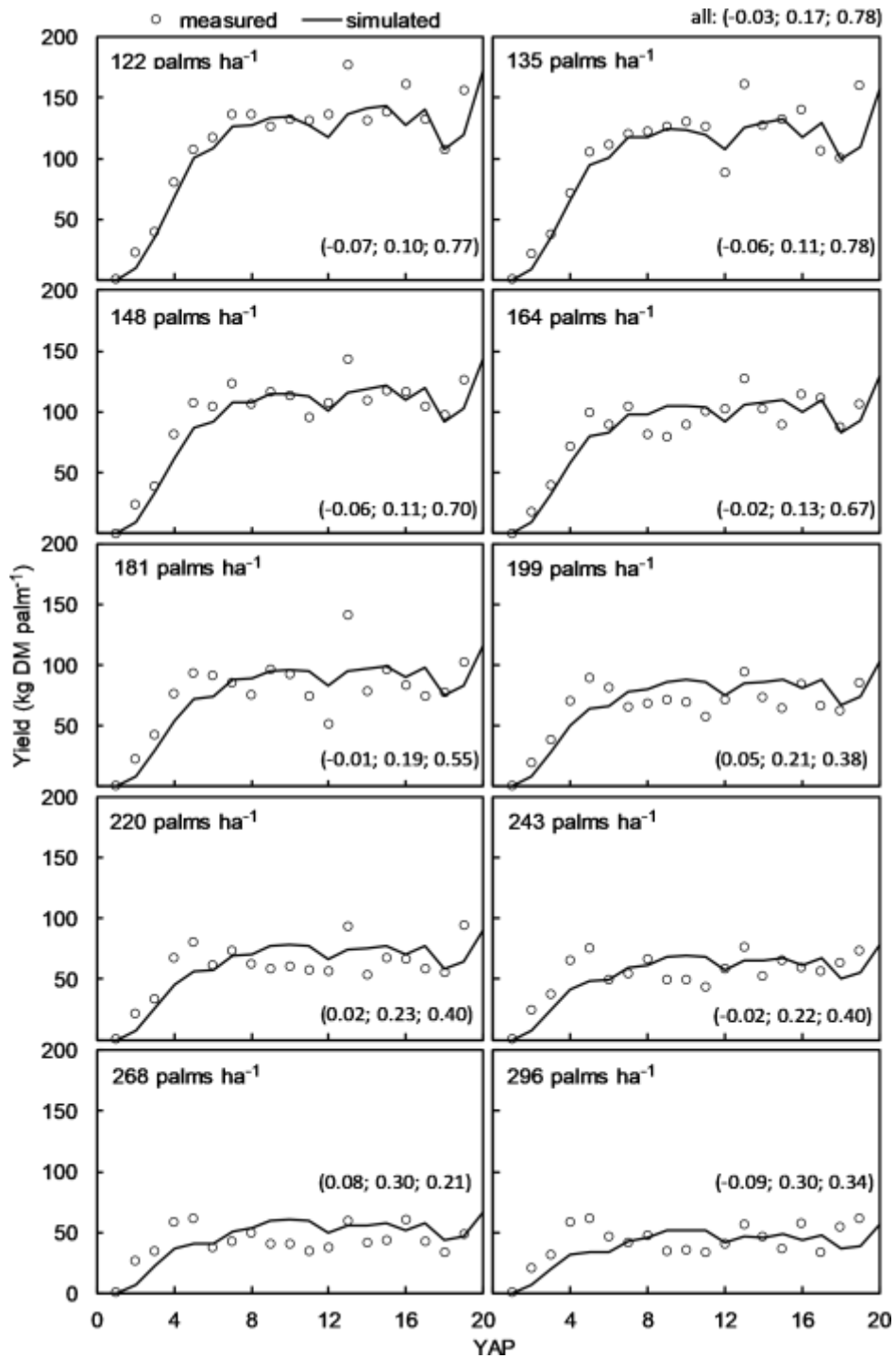


Fig. 10.11. Comparisons between model simulations and observations for fresh fruit bunch (FFB) yield. Year 11 and 18 are El Niño events. Values in brackets denote (NMBE, NMAE,  $d_r$ ), where NMBE is the normalized mean bias error, NMAE is the normalized mean absolute error, and  $d_r$  is the revised index of agreement. YAP is year after planting.

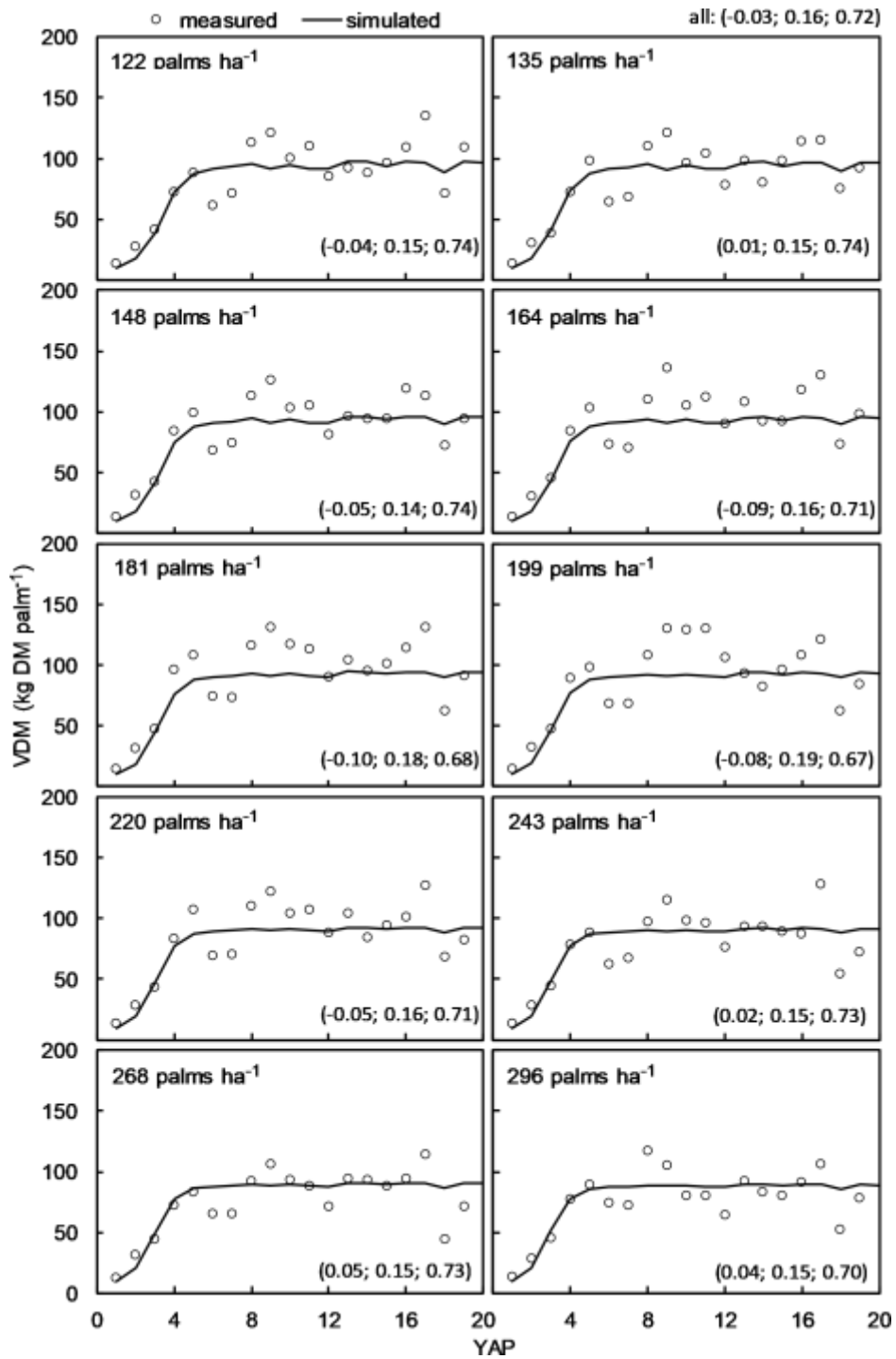


Fig. 10.12. Comparisons between model simulations and observations for aboveground vegetative dry matter (VDM). Values in brackets denote (NMBE, NMAE,  $d_r$ ), where NMBE is the normalized mean bias error, NMAE is the normalized mean absolute error, and  $d_r$  is the revised index of agreement. YAP is year after planting.

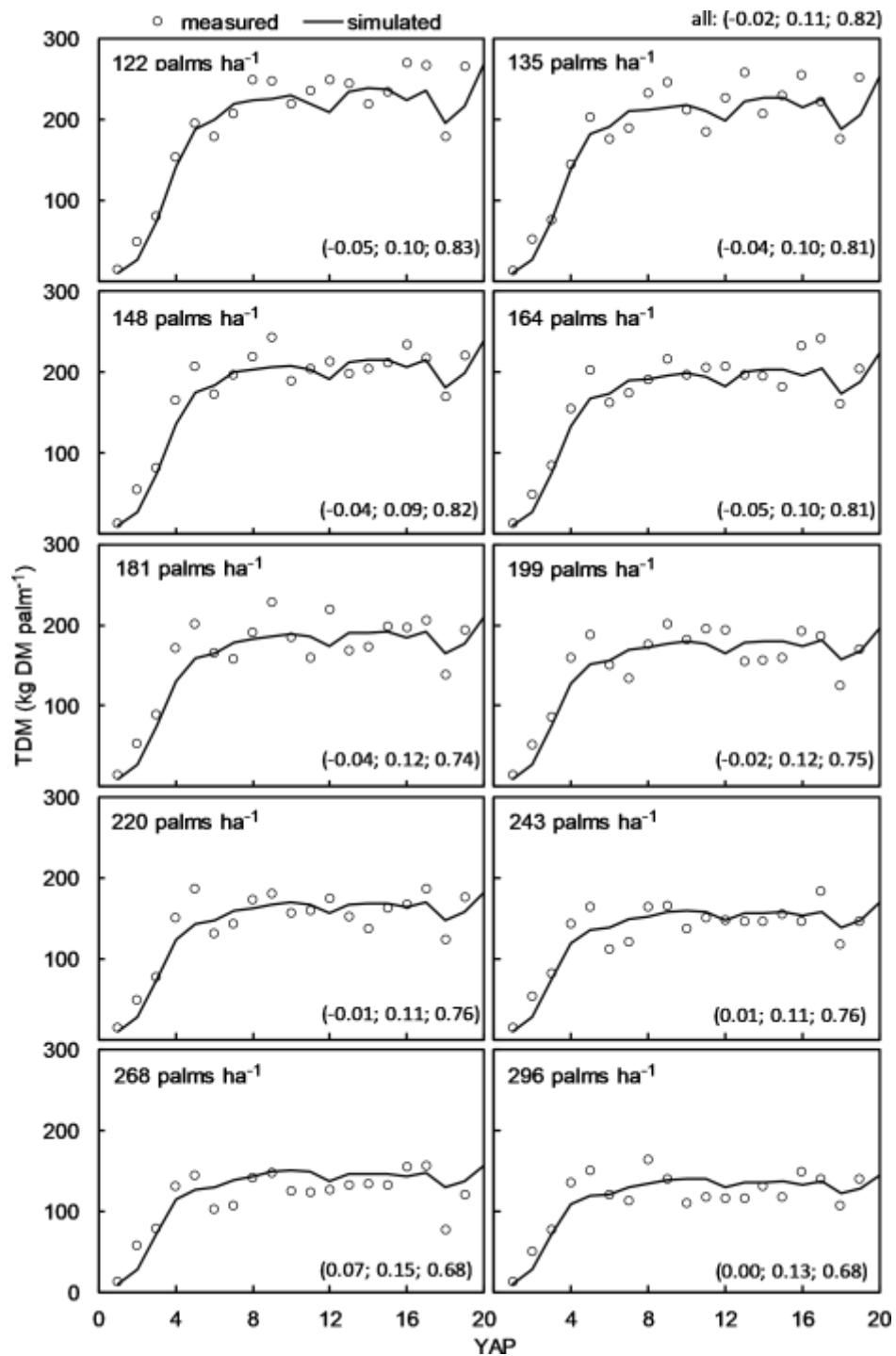


Fig. 10.13. Comparisons between model simulations and observations for total dry matter (TDM), which is the sum of yield and aboveground vegetative dry matter (VDM). Values in brackets denote (NMBE, NMAE,  $d_r$ ), where NMBE is the normalized mean bias error, NMAE is the normalized mean absolute error, and  $d_r$  is the revised index of agreement. YAP is year after planting.

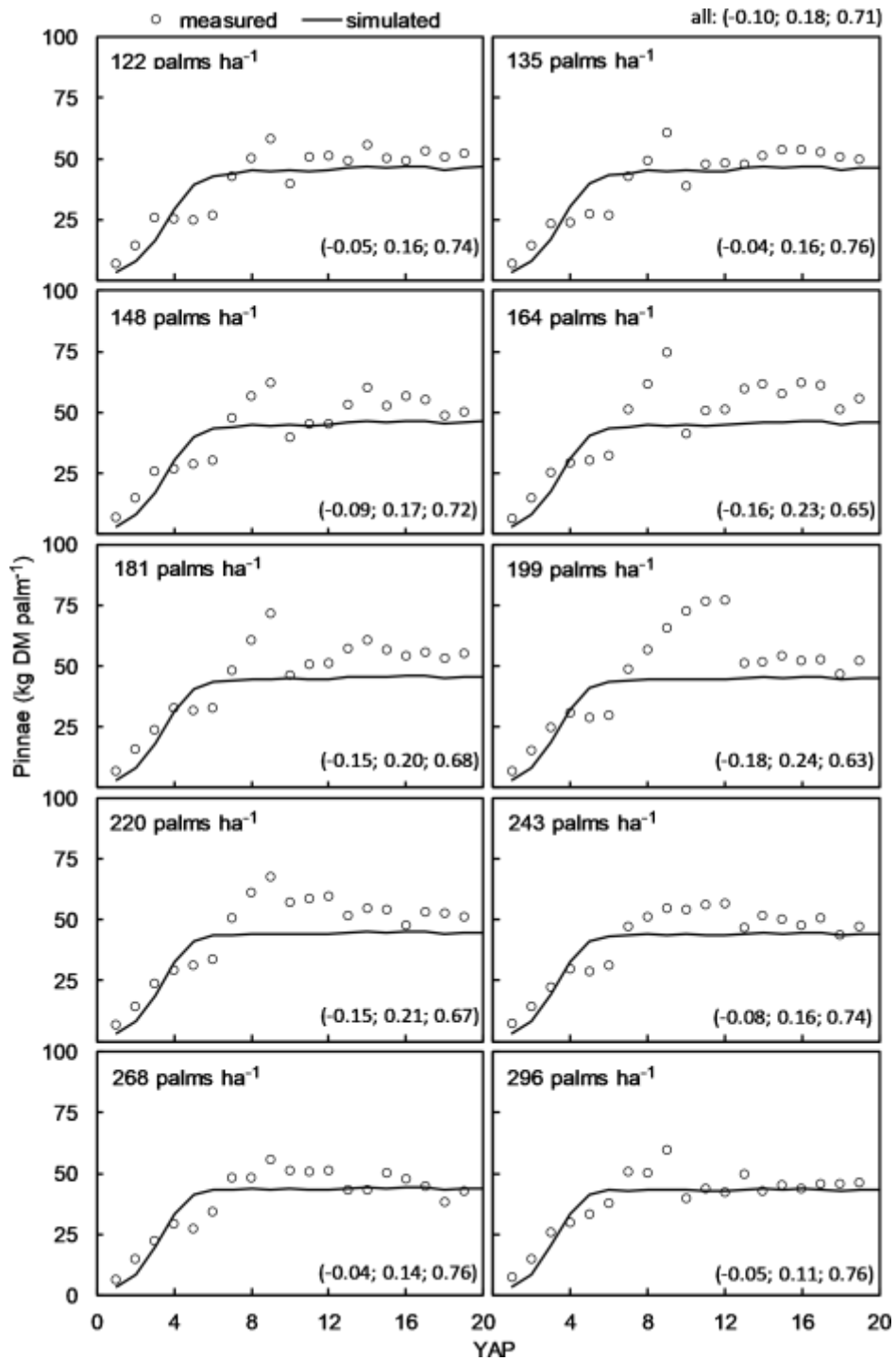


Fig. 10.14. Comparisons between model simulations and observations for pinnae biomass. Values in brackets denote (NMBE, NMAE,  $d_r$ ), where NMBE is the normalized mean bias error, NMAE is the normalized mean absolute error, and  $d_r$  is the revised index of agreement. YAP is year after planting.

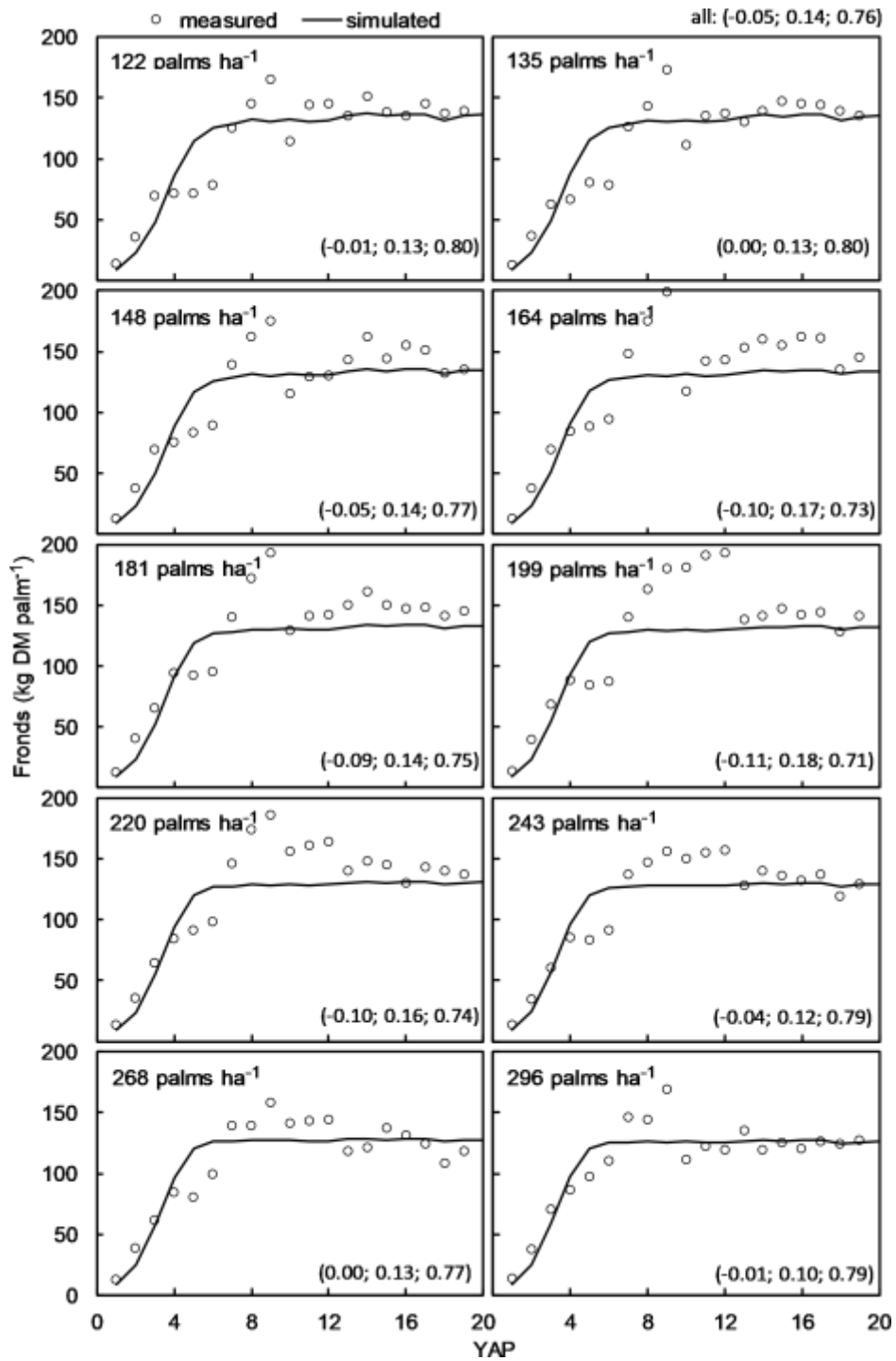


Fig. 10.15. Comparisons between model simulations and observations for fronds (pinnae and rachis) biomass. Values in brackets denote (NMBE, NMAE,  $d_r$ ), where NMBE is the normalized mean bias error, NMAE is the normalized mean absolute error, and  $d_r$  is the revised index of agreement. YAP is year after planting.

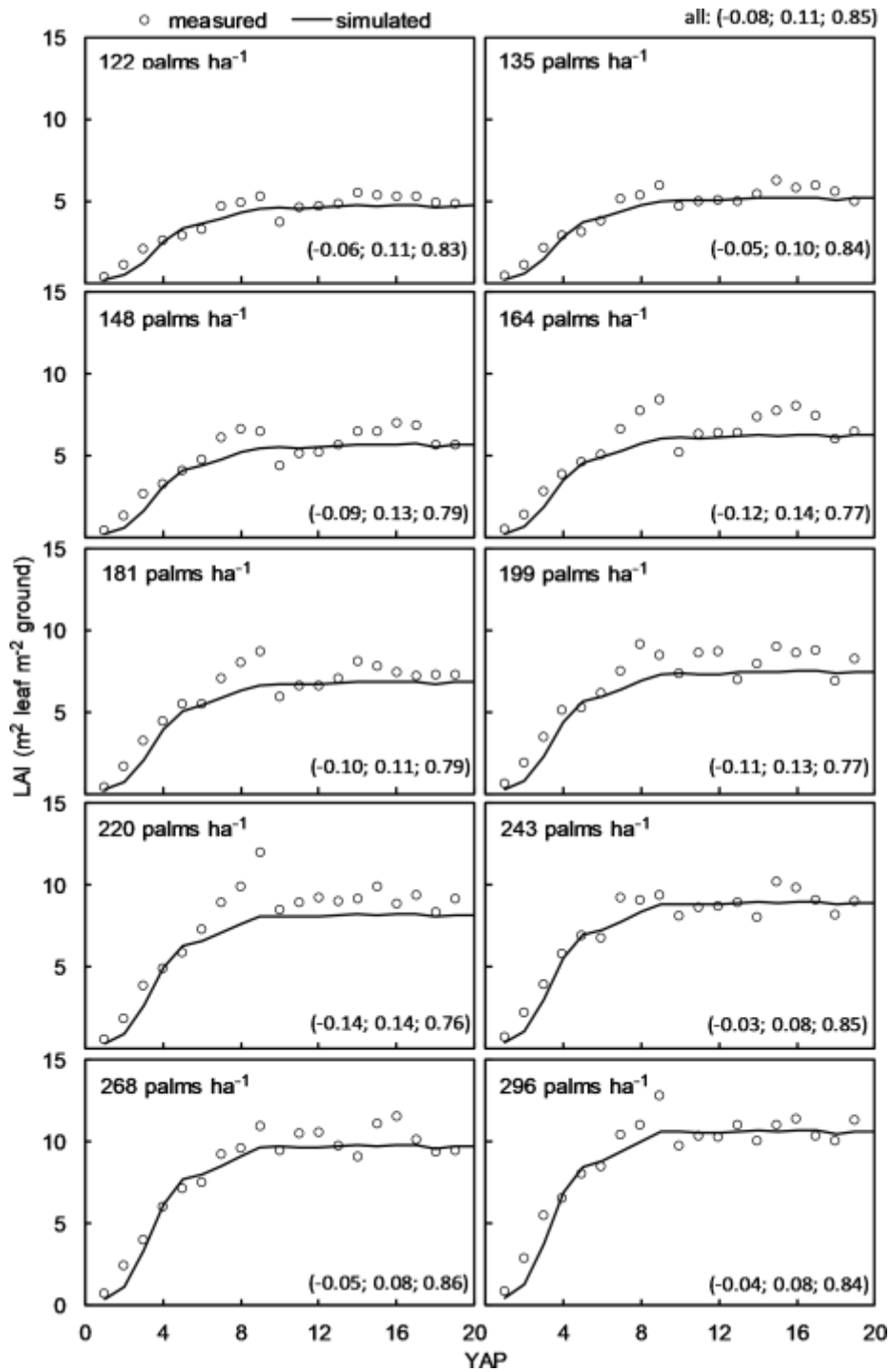


Fig. 10.16. Comparisons between model simulations and observations for total leaf area index (LAI). Values in brackets denote (NMBE, NMAE,  $d_r$ ), where NMBE is the normalized mean bias error, NMAE is the normalized mean absolute error, and  $d_r$  is the revised index of agreement. YAP is year after planting.

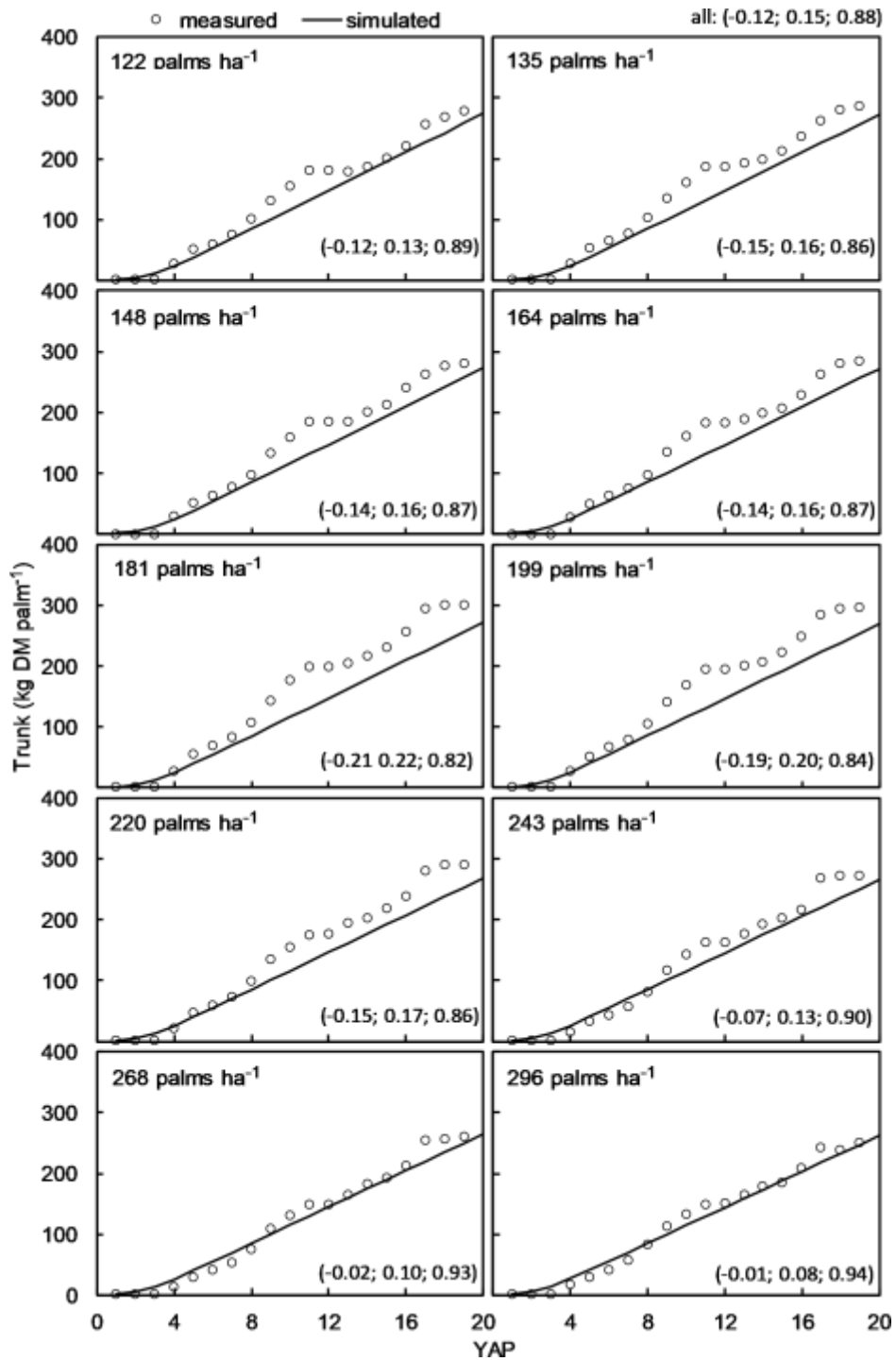


Fig. 10.17. Comparisons between model simulations and observations for standing trunk biomass. Values in brackets denote (NMBE, NMAE,  $d_r$ ), where NMBE is the normalized mean bias error, NMAE is the normalized mean absolute error, and  $d_r$  is the revised index of agreement. YAP is year after planting.

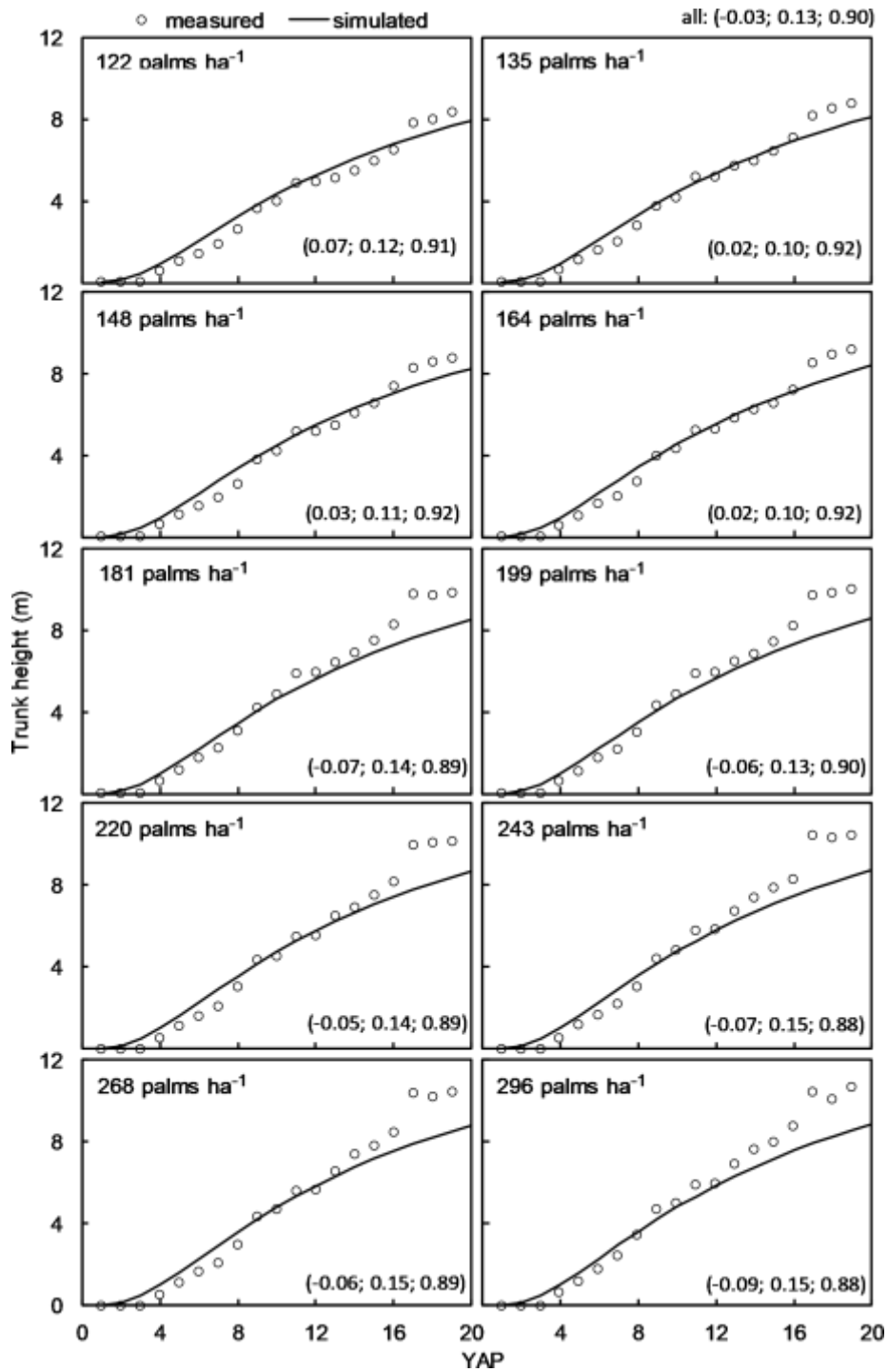


Fig. 10.18. Comparisons between model simulations and observations for trunk height. Values in brackets denote (NMBE, NMAE,  $d_r$ ), where NMBE is the normalized mean bias error, NMAE is the normalized mean absolute error, and  $d_r$  is the revised index of agreement. YAP is year after planting.

It is well established that crops in higher planting densities will produce lower yields and biomass on a per plant basis than in lower planting densities. Specifically for oil palm, PySawit

revealed that mean gross photosynthesis in PD122 was 878 kg CH<sub>2</sub>O palm<sup>-1</sup>, of which nearly two-thirds (65%) of the assimilates were used for total (maintenance and growth) respiration. The balance of the assimilates (35% or about 303 kg CH<sub>2</sub>O palm<sup>-1</sup>) was then available for flower and bunch development. But the mean gross photosynthesis in the highest planting density of PD296 was at a lower level of 624 kg CH<sub>2</sub>O palm<sup>-1</sup> (29% lower than in PD122), but total respiration consumed 83% of the assimilates, leaving only 17% (105 kg CH<sub>2</sub>O palm<sup>-1</sup>, which is about a third less than that used in PD122) for flower and bunch development.

There are several reasons for the lower gross photosynthesis in the higher than lower planting densities. One of which is the increase in the proportion of shaded to sunlit canopies in the higher planting densities compared with that in the lower planting densities. Increasing the proportion of shaded to sunlit canopies by 30%, for instance, lowers gross photosynthesis by nearly the same percentage (see Eq. 10.11). Increased leaf area in the higher planting densities would also increase the wind speed extinction coefficient; thus, reducing air flow within and below the canopies. In turn, this results in lower gas exchanges and lower photosynthetic rates.

Although much have been studied on oil palm, there remains considerable gaps in knowledge, one of which is the microclimate conditions under the oil palm canopies. Much less is known about the vertical wind speed profile and how soil water content and plant water uptake differ between oil palm planting densities. The accurate method of scaling up leaf to canopy conductance also needs to be studied in greater detail. Knowledge of these properties would allow oil palm models to better portray the daily variability of microclimate conditions under the oil palm canopies and to produce yield predictions that better match the variability or fluctuations in observed yields. That PySawit's yield prediction errors would become increasingly large for increasingly higher planting densities is indicative that the model's characterization of the microclimate conditions particularly under very dense canopies is still not representative enough. More work is also needed to determine the effects of planting density on the dry matter and nutrient content partitioning between the individual tree parts of oil palm.

#### **4. Conclusions**

An oil palm growth and yield model for crop production level 2 (where growth is only limited by weather conditions and water) was successfully developed. Model predictions generally agreed with observed values for several growth and yield parameters, and model accuracy was stable across all planting densities. Model predictions were especially good (small

discrepancies between predictions and observations and very little to none model bias) for TDM, LAI, and trunk height parameters. Yields decrease due to El Niño events were also reflected well in the model simulations. However, discrepancies between yield predictions and observations increased with increasing planting density. This is possibly because the microclimate conditions particularly under very dense canopies is not well understood and insufficiently characterized by the model. More work is also needed to determine the effects of planting density on soil water content, plant water use, and dry matter and nutrient content partitioning between the individual tree parts. Knowledge of these properties would further improve the model's accuracy and extend its range of applications.

PySawit was implemented as a computer program using Python computer language. The source code for PySawit can be downloaded from [www.christopherteh.com/pysawit](http://www.christopherteh.com/pysawit).

### **Acknowledgement**

The authors would like to thank Sime Darby Research Sdn. Bhd. for permission to use the oil palm trial and weather data for this modeling study.

### **5. References**

- Awal, M. A. (2008). Assessment of gap fraction by hemispherical photograph in oil palm plantation. *Suranaree Journal of Science and Technology*, 15, 233-241.
- Bentley, A. (2007). *Interception loss in Sedenak oil palm plantation*. B.Sc. final year project report. Skudai, Malaysia: Universiti Teknologi Malaysia.
- Bernacchi, C. J., Portis, A. R., Nakano, H., von Caemmerer, S., & Long, S. P. (2002). Temperature response of mesophyll conductance. Implication for the determination of Rubisco enzyme kinetics and for limitations to photosynthesis *in vivo*. *Plant Physiology*, 130, 1992–1998.
- Bernacchi, C. J., Singaas, E. L., Pimentel, C., Portis Jr., A. R., & Long, S. P. (2001). Improved temperature response functions for models of Rubisco-limited photosynthesis. *Plant, Cell and Environment*, 24, 253–259.
- Bittelli, M., Campbell, G. S., & Tomeu, F. (2015). *Soil physics with Python. Transport in the soil-plant-atmosphere system*. Oxford UK: Oxford University Press.

- Breure, C. J. (2003). The search for yield in oil palm: Basic principles. In T. H. Fairhurst & R. Härdter (Eds.), *Oil palm: management for large and sustainable yields* (pp. 59-98). Singapore: Potash & Phosphate Institute of Canada (ESEAP).
- Breure, C. J., & Powell, M. S. (1988). The one-shot method of establishing growth parameters in oil palm. In H. A. Halim, P. S. Chew & B. J. Wood (Eds.), *Proceedings of the 1987 International Oil Palm Conference. Progress and prospects* (pp. 203- 209). Kuala Lumpur, Malaysia: Palm Oil Research Institute of Malaysia.
- Brutsaert, W. (1982). *Evaporation into the atmosphere. Theory, history and applications*. Dordrecht, The Netherlands: D. Reidel Publishing Company.
- Campbell, G. S. (1994). *Soil physics with BASIC. Transport models for soil-plant systems*. Developments in Soil Science 14. Amsterdam, The Netherlands: Elsevier Science B.V.
- Campbell, G. S., & Norman, J. M. (1998). *An introduction to environmental biophysics* (2nd ed.). New York, NY: Springer-Verlag.
- Chong, S. Y. (2012). *Development of simple equations to estimate the net rainfall under closed tree canopies*. M. Agr. Sc. dissertation. Serdang, Malaysia: Universiti Putra Malaysia.
- Choudhury, B. J., & Monteith, J. L. (1988). A four-layer model for the heat budget of homogeneous land surfaces. *Quarterly Journal of the Royal Meteorological Society*, 114, 373-398.
- Collatz, G. T., Ball, J. T., Grivet, C., & Berry, J. A. (1991). Physiological and environmental - regulation of stomatal conductance, photosynthesis and transpiration: A model that includes a laminar boundary layer. *Agricultural and Forest Meteorology*, 54, 107-136.
- Combres, J. -C., Pallas, B., Rouan, L., Mialet-Serra, I., Caliman, J. -P., Braconnier, S., Soulié, J. -C., & Dingkuhn, M. (2012). Simulation of inflorescence dynamics in oil palm and estimation of environment-sensitive phenological phases: A model based analysis. *Functional Plant Biology*, 40, 263-279.
- Corley R. H. V., Ng, M., & Donough, C. R. (1995). Effects of defoliation on sex differentiation in oil palm clones. *Experimental Agriculture*, 31, 177–189.
- Corley, R. H. V., & Tinker, P. B. (2016). *The Oil Palm* (5th ed.). Chichester, UK: Wiley-Blackwell.

- Corley, R. H. V., Hardon, J. J., & Tan, G. Y. (1971). Analysis of growth of the oil palm (*Elaeis guineensis* Jacq.) I. Estimation of growth parameters and application in breeding. *Euphytica*, 20, 307-315.
- Damih, A. 1995. *Keberkesanan pemintasan air hujan oleh pokok kelapa sawit di dalam mengurangkan air larian permukaan* [Effectiveness of rainfall interception by oil palm trees in reducing surface runoff]. B.Sc. final year project report. Skudai, Malaysia: Universiti Teknologi Malaysia.
- de Wit, C. T., & Penning de Vries, F. W. T. (1982). L'Analyse des systemes de production primaire [Analysis of primary production systems]. In F. W. T. Penning de Vries & M. A. Djiteye (Eds.), *Une etude des sols, des vegetations et de l'exploitation de cette ressource naturelle* [A study of the soils, vegetations and exploitation of this natural resource] (pp. 20-27). Agricultural Research Reports 918. Wageningen, The Netherlands: Pudoc.
- Dimas, F. A., Gilani, S. I. H., & Aris, M. S. (2011). Hourly solar radiation estimation using ambient temperature and relative humidity data. *International Journal of Environmental Science and Development*, 2, 188-193.
- Dufrêne, E., & Saugier, B. (1993). Gas exchange of oil palm in relation to light, vapour pressure deficit, temperature and leaf age. *Functional Ecology*, 7, 97-104
- Dufrêne, E., Ochs, R., & Saugier, B. (1990). Oil palm photosynthesis and productivity linked to climatic factors. *Oléagineux*, 45, 345-355.
- Ephrath, J. E., Goudriaan, J., & Marani, A. (1996). Modelling diurnal patterns of air temperature, radiation, wind speed and relative humidity by equations from daily characteristics. *Agricultural Systems*, 51, 377-393.
- Fan, Y., Rouspard, O., Bernoux, M., Le Maire, G., Panferov, O., Kotowska, M. M., & Knohl, A. (2015). A sub-canopy structure for simulating oil palm in the Community Land Model (CLM-Palm): phenology, allocation and yield. *Geoscientific Model Development*, 8, 3785-3800.
- Farahani, H. J., & Ahuja, L. R. (1996). Evapotranspiration modeling of partial canopy/residue-covered fields. *Transactions of the ASAE*, 39, 2051-2064.
- Farquhar, G. D., von Caemmerer, S., & Berry, J. A. (1980). A biochemical model of photosynthetic CO<sub>2</sub> assimilation in leaves of C<sub>3</sub> species. *Planta*, 149, 78-90.

- Foong, F. S. (1999). Impact of moisture on potential evapotranspiration, growth and yield of oil palm. In D. Arifin, K. W. Chan & S. R. S. A. Sharifah (Eds.), *Proceedings of the 1999 PORIM International Palm Oil Congress (Agriculture)* (pp. 265-287). Bangi, Malaysia: Palm Oil Research Institute of Malaysia.
- Gerritsma, W. (1988). *Simulation of oil palm yield*. Report. Department of Theoretical Production Ecology. Wageningen, The Netherlands: Wageningen Agricultural University.
- Goudriaan, J. (1977). *Crop micrometeorology: A simulation study*. Simulation Monograph. Pudoc, Wageningen: Centre for Agricultural Publishing and Documentation.
- Goudriaan, J., & van Laar, H. H. (1994). *Modeling potential crop growth processes. A textbook with exercise*. Current issues in production ecology. Dordrecht, The Netherlands: Kluwer Academic Publishers.
- Hansen, F. V. (1993). *Surface roughness lengths*. ARL Technical Report. White Sands Missile Range, NM 88002-5501: U.S. Army.
- Hardon J. J., Williams C. N., & Watson I. (1969). Leaf area and yield in the oil palm in Malaya. *Experimental Agriculture*, 5, 25-32.
- Hasanuzzaman, M., Nahar, K., Alam, M. M., Roychowdhury, R., & Fujita, M. (2013). Extreme temperature responses, oxidative stress and antioxidant defense in plants. In K. Vahdat & C. Leslie (Eds.), *Abiotic Stress - Plant Responses and Applications in Agriculture* (pp. 169-205). Vienna, Austria: InTech.
- Henry, P. (1955). Leaf growth morphology in *Elaeis*. *Revue Generale de Botanique*, 32, 66-67.
- Henson, I. E. (1989). *Modelling gas exchange, yield and conversion efficiency*. Workshop on Productivity of Oil Palm. Bangi, Malaysia: Palm Oil Research Institute of Malaysia.
- Henson, I. E. (1995). Carbon assimilation, water use and energy balance of an oil palm plantation assessed using micrometeorological techniques. In S. Jalani, D. Ariffin, N. Rajanaidu, D. Mohd Tayeb, K. Paranjothy, W. Mohd Basri, I. E. Henson & C. K. Chan (Eds.), *Proceedings of the 1993 PORIM International Palm Oil Congress - Update and Vision (Agriculture)* (pp. 137-158). Bangi, Malaysia: Palm Oil Research Institute of Malaysia.
- Henson, I. E. (2000). Modelling the effects of 'haze' on oil palm productivity and yield. *Journal of Oil Palm Research*, 12, 123-134.

- Henson, I. E. (2009). Modelling dry matter production, partitioning and yield of oil palm. OPRODSIM: A mechanistic simulation model for teaching and research. Technical manual and users' guide. Kuala Lumpur, Malaysia: Malaysian Palm Oil Board.
- Henson, I. E., & Chai, S. (1997). Analysis of oil palm productivity. II. Biomass, distribution, productivity and turnover of the root system. *Elaeis*, 9, 78-92.
- Henson, I. E., & Mohd Tayeb, D. (2003). Physiological analysis of an oil palm density trial on a peat soil. *Journal of Oil Palm Research*, 15, 1-27.
- Hoffmann, M. P., Castaneda Vera, A., van Wijk, M. T., Giller, K. E., Oberthür, T., Donough, C., & Whitbread, A. M. (2014). Simulating potential growth and yield of oil palm (*Elaeis guineensis*) with PALMSIM: Model description, evaluation and application. *Agricultural Systems*, 131,1-10.
- Huth, N.I., Banabas, M., Nelson, P. N., & Webb, M. (2014). Development of an oil palm cropping systems model: lessons learned and future directions. *Environmental Modelling & Software*, 62, 411-419.
- Jacquemard, J. C. (1979). Contribution to the study of the height growth of the stems of *Elaeis guineensis* Jacq. Study of the L2T x D10D cross. *Oléagineux*, 34, 492-497.
- Jacquemard, J. C. (1998). *Oil palm*. London, UK: Macmillan Education Ltd.
- Jourdan, C., & Rey, H. (1997). Architecture and development of the oil-palm (*Elaeis guineensis* Jacq.) root system. *Plant and Soil*, 189, 33-48.
- Kallarackal, J., Jeyakumar, P., & George, S. J. (2004). Water use of irrigated oil palm at three different arid locations in Peninsular India. *Journal of Oil Palm Research*, 16, 45-53.
- Kropff, M. J. (1993). Mechanisms of competition for light. In M. J. Kropff & H. H. van Laar (Eds.), *Modelling crop-weed interactions* (pp. 33-61). Wallingford, UK: CAB International (in association with International Rice Research Institute).
- Kustas, W. P., & Daughtry, C. S. T. 1990. Estimation of the soil heat flux/net radiation ratio from spectral data. *Agriculture and Forest Meteorology*, 49, 205-223.
- Kustas, W. P., & Norman, J. M. (1999). Evaluation of soil and vegetation heat flux predictions using a simple two-source model with radiometric temperatures for partial canopy cover. *Agricultural and Forest Meteorology*, 94, 13-29.

- Kwan, B. K. W. (1994). *The effect of planting density on the first fifteen years of growth and yield of oil palm in Sabah*. Technical Bulletin No. 11. Kota Kinabalu, Malaysia: Department of Agriculture, Sabah.
- Liu, B.Y., & Jordan, R.C. (1960). The interrelationship and characteristic distribution of direct, diffuse, and total solar radiation. *Solar Energy*, 4, 1-19.
- Long, S. P., & Bernacchi, C. J. (2003). Gas exchange measurements, what can they tell us about the underlying limitations to photosynthesis? Procedures and sources of error. *Journal of Experimental Botany*, 54, 2393-2401.
- Lubis, M. E. S. (2016). *Water dynamics and groundwater quality assessment in an oil palm ecosystem*. Ph.D. dissertation. Serdang, Malaysia: Universiti Putra Malaysia.
- Massman, W. J. (1987). A comparative study of some mathematical models of the mean wind structure and aerodynamic drag of plant canopies. *Boundary-Layer Meteorology*, 40, 179-197.
- Massman, W. J. (1997). An analytical one-dimensional model of momentum transfer by vegetation of arbitrary structure. *Boundary-Layer Meteorology*, 83, 407-421.
- Miyazaki, T. (2005). *Water flow in soils*. Boca Raton, FL: CRC Press.
- Mohd. Desa, M. N., & Rakhecha, P. R. (2006). Deriving the highest persisting monthly 24-hour dew points in Malaysia for the estimation of PMP. In S. Demuth, A. Gustard, E. Planos, F. Scatena & E. Servat (Eds.), *Climate Variability and Change-Hydrological Impacts. Proceedings of the Fifth FRIEND World Conference held at Havana, Cuba, November 2006*. IAHS Publ. 308 (pp. 287-293). Wallingford, UK: International Association of Hydrological Sciences (IAHS).
- Monteith, J. L. (1965). Evaporation and the environment. *Symposium of the Society of Experimental Biology*, 19, 205-234.
- Monteith, J. L. (1973). *Principles of environmental physics*. London, UK: Edward Arnold.
- Nelson, P. N., Banabas, M., Scotter, D.R., & Webb, M. J. (2006). Using soil water depletion to measure spatial distribution of root activity in oil palm (*Elaeis guineensis* Jacq.) plantations. *Plant Soil*, 286, 109-121.

- Nikolov, N., & Zeller, K. F. (2003). Modeling coupled interactions of carbon, water, and ozone exchange between terrestrial ecosystems and the atmosphere. I: Model description. *Environmental Pollution*, 124, 231-246.
- Paterson, R. R. M., Kumar, L., Taylor, S., & Lima, N. (2015). Future climate effects on suitability for growth of oil palms in Malaysia and Indonesia. *Scientific Reports*, 5, 1–11.
- Rao, V., Rajanaidu, N., Kushairi, A., & Jalani, S. (1992). Density effect in the oil palm. In *Proceedings in the ISOP International Workshop of Yield Potential in the Oil Palm* (pp. 71-79). Bangi, Malaysia: International Society for Oil Palm Breeders and PORIM.
- Rey, H., Quencez, P., Dufrêne, E., & Dubos, B. (1998). Oil palm water profiles and water supplies in Côte d'Ivoire. *Plantations, Recherche, Développement*, 5, 47- 57.
- Saxton, K. E., & Rawls, W. J. (2006). Soil water characteristic estimates by texture and organic matter for hydrologic solutions. *Soil Science Society of America Journal*, 70, 1569-1578.
- Sharkey, T. D. (2015). What gas exchange data can tell us. *Plant, Cell & Environment*, 39, 1161-1163.
- Sharkey, T. D., Bernacchi, C. J., Farquhar, G. D., & Singsaas, E. L. (2007). Fitting photosynthetic carbon dioxide response curves for C3 leaves. *Plant, Cell and Environment*, 30, 1035-1040.
- Shen, L., & Chen, Z. (2007). Critical review of the impact of tortuosity on diffusion. *Chemical Engineering Science*, 62, 3748-3755.
- Shuttleworth, W. J., & Wallace J. S. (1985). Evaporation from sparse crops - an energy combination theory. *Quarterly Journal of the Royal Meteorological Society*, 111, 839-855.
- Skillman, J. B. (2008). Quantum yield variation across the three pathways of photosynthesis: Not yet out of the dark. *Journal of Experimental Botany*, 59, 1647-1661.
- Sopian, K., Hj. Othman, M. Y., & Wirsat, A. (1995). Data bank. The wind energy potential of Malaysia. *Renewable Energy*, 6, 1005-1016.
- Su, Z., Schmugge, T., Kustas, W., & Massman, W. (2001). An evaluation of two models for estimation of the roughness height for heat transfer between the land surface and the atmosphere. *Journal of Applied Meteorology*, 40, 1933-1951.

Szeicz, G., & Long, I. F. (1969). Surface resistance of crop canopies. *Water Resources Research*, 5, 622-633.

Tan, Y. P., & Ng, S. K. (1977). Spacing for oil palms on coastal clays in Peninsular Malaysia. In D. A. Earp & W. Newall (Eds.), *International Developments in Oil Palm. Proceedings of the Malaysian International Agricultural Oil Palm Conference* (pp. 183-191). Kuala Lumpur, Malaysia: Incorporated Society of Planters.

Teh, C. B. S. (2006). *Introduction to mathematical modeling of crop growth: How the equations are derived and assembled into a computer program*. Boca Raton, FL: Brown Walker Press.

Thornley, J. H. M. (1970). Respiration, growth and maintenance in plants. *Nature*, 227, 304-305.

van Keulen, H., & Seligman, N. G. (1987). *Simulation of water use, nitrogen and growth of a spring wheat crop*. Simulation Monographs. Wageningen, The Netherlands: Pudoc.

van Kraalingen, D. W. G. (1985). *Simulation of oil palm growth and yield*. Ph.D. thesis. Wageningen, The Netherlands: Wageningen Agricultural University.

van Kraalingen, D. W. G., Breure, C. J., & Spitters, C. J. T. (1989). Simulation of oil palm growth and yield. *Agricultural and Forest Meteorology*, 46, 227-244.

van Noordwijk, M., Lusiana, B., Khasanah, N., & Mulia, R. (2011). WaNuLCAS 4.0: Background on a model of water, nutrient, and light capture in agroforestry systems. Bogor, Indonesia: World Agroforestry Centre (ICRAF).

Wilkerson, G. G., Jones, J. W., Boote, K. J., Ingram, K. T., & Mishoe, J. W. (1983). Modeling soybean growth for crop management. *Transactions of the ASAE*, 26, 63-73.

Willmott C. J., Robeson S. M., & Matsuura, K. (2012). A refined index of model performance. *International Journal of Climatology*, 32, 2088-2094.

Yin, X., & van Laar, H. H. (2005). *Crop systems dynamics. An ecophysiological simulation model for genotype-by-environment interactions*. Wageningen, The Netherlands: Wageningen Academic Publishers.

Yu, S., Eder, B., Dennis, R., Chu, S. -H., & Schwartz, S. E. (2006). New unbiased symmetric metrics for evaluation of air quality models. *Atmospheric Science Letters*, 7, 26-34.

Zulkifli, Y., Geoffery, J., Saw, A. L., & Norul, S. T. (2006). Preliminary study on throughfall spatial variability and stemflow characteristics under oil palm catchment. In *Proceedings of the National Water Conference (in CD)*. Kuala Lumpur, Malaysia: Malaysian Hydrological Society.

## List of main symbols

Symbol	Description	Units
$\gamma$	psychometric constant (0.658)	mbar K <sup>-1</sup>
$\Gamma^*$	CO <sub>2</sub> compensation point	μmol CO <sub>2</sub> mol <sup>-1</sup> air
$\Delta$	slope of the saturated vapor pressure curve	mbar K <sup>-1</sup>
$\theta$	solar inclination (from vertical)	radians
$\theta$	volumetric soil water content	m <sup>3</sup> m <sup>-3</sup>
$\theta_{0/33/1500}$	volumetric soil water content at saturation (0), field capacity (33), or permanent wilting point (1500)	m <sup>3</sup> m <sup>-3</sup>
$\theta_{root}$	volumetric soil water content in the root zone	m <sup>3</sup> m <sup>-3</sup>
$\theta_{cr}$	critical volumetric soil water content	m <sup>3</sup> m <sup>-3</sup>
$\Theta_i$	soil water content	m
$\lambda$	pore-size distribution index	-
$\lambda ET$	total latent heat flux density	W m <sup>-2</sup>
$\lambda ET_{c/s}$	latent heat flux density of crop (c) or soil (s)	W m <sup>-2</sup>
$\Lambda_{canopy}$	instantaneous gross canopy assimilation	μmol CO <sub>2</sub> m <sup>-2</sup> ground s <sup>-1</sup>
$\Lambda_{canopy,d}$	daily gross canopy assimilation	kg CH <sub>2</sub> O palm <sup>-1</sup> day <sup>-1</sup>
$\Lambda_{sl/sh}$	gross leaf assimilation rate of CO <sub>2</sub> for sunlit (sl) or shaded (sh) leaves	μmol CO <sub>2</sub> m <sup>-2</sup> leaf s <sup>-1</sup>
$\rho_{df/dr}$	reflection coefficient for diffuse (df) or direct photosynthetically active radiation (PAR)	-
$\rho_{cp}$	volumetric heat capacity of air (1221.09)	J m <sup>-3</sup> K <sup>-1</sup>
$\tau$	CO <sub>2</sub> / O <sub>2</sub> specificity factor	μmol O <sub>2</sub> μmol <sup>-1</sup> CO <sub>2</sub>
$\tau$	atmospheric transmittance (sky clearness)	-
$\tau$	soil tortuosity	-
$\tau_b$	canopy gap fraction	-
$\phi_p$	soil porosity	m <sup>3</sup> m <sup>-3</sup>
$\omega, \omega_0$	canopy clustering coefficient at current sun position and at when the sun is at zenith, respectively	-
<i>age</i>	tree age	days
<i>A</i>	total energy supply to crop and soil	W m <sup>-2</sup>

<b>Symbol</b>	<b>Description</b>	<b>Units</b>
$A_{c/s}$	energy available to the crop (c) or soil (s)	$W m^{-2}$
$C_{a/i}$	CO <sub>2</sub> concentration in ambient air (a) and within stomata (i)	$\mu mol CO_2 mol^{-1} air$
$CVF, CVF_2$	conversion from CH <sub>2</sub> O to dry (DM) weight	$kg DM kg^{-1} CH_2O$
$d$	zero plane displacement	m
$d_{root}$	rooting depth	m
$d_{groot}$	rooting depth growth rate	$m day^{-1}$
$D$	air vapor pressure deficit (VPD)	mbar
$D_{0/leaf}$	air VPD at mean canopy flow (0) or leaf VPD (leaf)	mbar
$DL$	day length	hour
$DM_{(part)}$	fraction of dry matter to a given plant part	-
$e_a$	air vapor pressure	mbar
$e_m$	quantum efficiency or yield (0.051)	$\mu mol CO_2 \mu mol^{-1} photons$
$e[[T]]$	saturated vapor pressure at temperature $T$	mbar
$ET_{c/s}$	potential transpiration (c) or evaporation (s)	$m day^{-1}$
$f_{D/PAR/water}$	reduction of stomatal conductance due to VPD (D), low PAR, or water stress (water)	-
$gst, gst_{max}$	current and maximum stomatal conductance, respectively	$m s^{-1}$
$G$	soil (ground) heat flux density	$W m^{-2}$
$G_{death,(part)}$	death rate of a given plant part	$kg DM palm^{-1} day^{-1}$
$G_{gen}$	total assimilates available for generative organs growth	$kg CH_2O palm^{-1} day^{-1}$
$G_{gen, (part)}$	growth rate of a given generative organ	$kg DM palm^{-1} day^{-1}$
$G_{growth}$	total assimilates available for growth respiration	$kg CH_2O palm^{-1} day^{-1}$
$G_{growth, (part)}$	growth rate of a given plant part	$kg DM day^{-1}$
$h$	tree height (trunk + canopy)	m
$h_{canopy}, h_{trunk}$	canopy and trunk height, respectively	m
$h'_{trunk}$	rate of growth for trunk height	$m day^{-1}$
$H$	total head (matric and gravity)	m

<b>Symbol</b>	<b>Description</b>	<b>Units</b>
$H$	total sensible heat density	$W m^{-2}$
$H_{c/s}$	sensible heat flux density of crop (c) or soil (s)	$W m^{-2}$
$I_{df/dr}$	diffuse (df) or direct (dr) solar irradiance	$W m^{-2}$
$I_{et}, I_t$	extraterrestrial and total solar irradiance, respectively	$W m^{-2}$
$k$	von Karman's constant (0.4)	-
$k_{df/dr}$	canopy extinction coefficient for diffuse (df) or direct (dr) solar radiation	-
$k_{e/w}$	extinction coefficient for eddy diffusivity (e) or wind speed (w)	-
$K_{\theta}, \overline{K_{\theta}}$	unsaturated and mean hydraulic conductivity, respectively	$m day^{-1}$
$K_{c/o}$	Michaelis-Menten constant for $CO_2$ (c) or $O_2$ (o)	$\mu mol CO_2/O_2 mol^{-1} air$
$L, L_{eff}$	total and effective leaf area index, respectively	$m^2 leaf m^{-2} ground$
$L_{sh/sl}$	shaded (sh) or sunlit (sl) leaf area index	$m^2 leaf m^{-2} ground$
$L_{max,PD}$	maximum leaf area index for a given planting density	$m^2 leaf m^{-2} ground$
$m$	optical mass number	-
$M_{(part)}$	maintenance respiration for a given plant part	$kg CH_2O palm^{-1} day^{-1}$
$N_{(part)}$	fraction by weight of nitrogen content in given plant part	-
$O_a$	air ambient concentration of $O_2$	$\mu mol O_2 mol^{-1} air$
$PD$	planting density	$palms ha^{-1}$
$P_g, P_{net}$	gross and net daily rainfall, respectively	m
$q$	water flux	$m day^{-1}$
$\hat{q}$	net water flux	$m day^{-1}$
$Q_{df/dr}$	diffuse (df) or diffuse (df) PAR component	$\mu mol m^{-2} leaf s^{-1}$
$Q_{sh/sl}$	total PAR absorbed by shaded (sh) or sunlit (sl) leaves	$\mu mol m^{-2} leaf s^{-1}$
$Q_{10}$	relative change for every 10 °C change	-

<b>Symbol</b>	<b>Description</b>	<b>Units</b>
$\overline{Q_{p,df}}$	mean diffuse PAR component (within canopies)	$\mu\text{mol m}^{-2} \text{ ground s}^{-1}$
$Q_{p,dr}$	unintercepted direct PAR component (with scattering component) (within canopies)	$\mu\text{mol m}^{-2} \text{ leaf s}^{-1}$
$Q_{p,dr,\alpha}$	scattered PAR component only (within canopies)	$\mu\text{mol m}^{-2} \text{ ground s}^{-1}$
$Q_{p,dr,dr}$	unintercepted direct PAR component (without scattering component) (within canopies)	$\mu\text{mol m}^{-2} \text{ leaf s}^{-1}$
$r_a^a$	aerodynamic resistance between the mean canopy flow and reference height	$\text{s m}^{-1}$
$r_a^c$	bulk boundary layer resistance	$\text{s m}^{-1}$
$r_s^c$	canopy resistance	$\text{s m}^{-1}$
$r_a^s$	aerodynamic resistance between the soil surface and mean canopy flow	$\text{s m}^{-1}$
$r_s^s$	soil surface resistance	$\text{s m}^{-1}$
$R_n, R_{nL}$	net solar radiation and net longwave radiation, respectively	$\text{W m}^{-2}$
$R_{Ds}, R_{Dc}$	reduction factor for evaporation and transpiration, respectively	-
$RH$	relative humidity	%
$SLA$	specific leaf area	$\text{m}^2 \text{ leaf kg}^{-1} \text{ DM}$
$t_h$	local solar hour	hour
$t_{sr}, t_{ss}$	local solar hour for sunrise and sunset, respectively	hour
$T_a, T_{dew}, T_f$	air, dew point, and foliage temperature, respectively	$^{\circ}\text{C}$
$T_{min/max}$	minimum (min) or maximum (max) air temperature	$^{\circ}\text{C}$
$u^*$	friction velocity	$\text{m s}^{-1}$
$u, u_d, u_h$	wind speed, mean daily wind speed, and wind speed at canopy height, respectively	$\text{m s}^{-1}$
$u_{min/max}$	minimum (min) or maximum (max) daily wind speed	$\text{m s}^{-1}$

<b>Symbol</b>	<b>Description</b>	<b>Units</b>
$V_c/q/s$	CO <sub>2</sub> assimilation limited by Rubisco (c), light (q), or sink (s)	$\mu\text{mol CO}_2 \text{ m}^{-2} \text{ leaf s}^{-1}$
$V_{cmax}$	Rubisco capacity rate	$\mu\text{mol CO}_2 \text{ m}^{-2} \text{ leaf s}^{-1}$
$VDM,$ $VDM_{max,PD}$	current and maximum vegetative dry matter requirement for a given planting density, respectively	$\text{kg DM palm}^{-1} \text{ yr}^{-1}$
$w$	mean pinnae width	m
$W_{(part)}$	dry weight of a given plant part	$\text{kg DM palm}^{-1}$
$X_{(part)}$	fraction by weight of mineral content in a given plant part	-
$z_0/s_0$	crop (0) or soil surface (s0) roughness length	m
$z_r$	reference height	m